2.5. Immunohistochemical analysis

Although histologic diagnosis was made based on H&E staining, immunohistochemical analyses were performed to characterize cells. Four-micrometer-thick tissue sections were mounted on silane-coated slides, routinely deparaffinized in xylene, and rehydrated through graded ethanol. For antigen retrieval, the slides were heated at 97°C for 40 minutes in citrate buffer at pH 6.0 or in EDTA buffer at pH 9.0. Immunohistochemical staining was performed using the EnVision+ DAB system with an autostainer (Dako, Glostrup, Denmark). Endogenous peroxidase activity was blocked with 3% hydrogen peroxide in methanol, and then each antibody was applied (Supplementary Table 1). We used antibodies for synaptophysin (SYP), chromogranin A (CGA), and CD56 as NE markers, as well as antibodies for p63 and high-molecular-weight cytokeratin (clone 34βE12 or K903) as basal cell markers (BA). Particular attention was paid to judgment of immunoreactivity in surgical materials because we intended to make a comparison between surgical and biopsy materials. Specifically, to avoid false-negative judgments in surgical materials, we always confirmed that positive control cells were correctly stained. Immunoreactivity was scored based on the percentage of cells that stained positively: negative, 0; less than 10%, 1+; 10% to 50%, 2+; and more than 50%, 3+. Only foci with SCLC morphology were evaluated if the case was diagnosed as combined with non-SCLC. The expression of each antibody in a tumor was defined as positive when 10% of the tumor cells or greater were stained (scores 2+ and 3+) and negative when less than 10% were stained (scores 0 and 1+). We defined cases with either positive p63 or CK34βE12 as belonging to the BA+ group and cases with any one of positive SYP, CGA, or CD56 as the NE+ group. Accordingly, all cases were divided into 4 groups: NE+BA−, NE+BA+, NE−BA+, and NE−BA−. Two independent observers (W. H. and Y. I.) pathologically reviewed all slides without any prior knowledge of patients, and discrepancies were resolved by joint discussion of the slides viewed with a multiheaded microscope.

2.6. Analysis of clinicopathological parameters

All analyses were performed using GraphPad PRISM software (ver 5.0b for Macintosh; GraphPad Software, San Diego, CA, USA) and SPSS software (ver 15.0; SPSS, Chicago, IL). We analyzed statistical correlations for clinicopathological features using the χ^2 test with Yate correction. Survival curves were delineated by Kaplan-Meier method, and survival difference was tested by the log-rank test using overall survival or cancer-specific survival, as appropriate. We also conducted univariate and multivariate analyses of the prognostic factors using the Cox proportional hazards model. All differences were considered statistically significant if $P < .05$.

3. Results

3.1. Gene expression analysis by microarray

To validate the results of the previous study with our cDNA microarray, 30 SCLCs were enrolled for the current study. The clinical characteristics of the enrolled cases were as follows: 21 men and 9 women; average age, 67 years; 27 (90%) were smokers; the median tumor size was 31 mm; and 14 (47%) were at p-stage I.

Unsupervised hierarchical clustering was performed with 15 431 of 54 000 probe sets on oligonucleotide array chips (Affymetrix HG U133 plus 2.0) expressed stably among all samples. The result of this clustering is shown in Fig. 1A. We obtained again 2 clusters, groups 1 and 2, and cases in group 2 had significantly better survival ($P = .0014$; Fig. 1B). We compared which genes were differently expressed in these 2 groups (Supplementary Table 2). Cases in group 2 highly expressed genes related to cell growth (G protein-coupled receptor, cyclin D1, *MYC*, etc), but many genes related to NE differentiation (*ASCL1*, *GRP*, *NCAM* [*CD56*], *CHGA*) were down-regulated.

3.2. Clinical characteristics of SCLC surgical patients and inoperable patients

As detailed in Table 1, for the surgical patients, the male/female ratio was 34:9, with a median age of 67 years (range, 46-84 years). Forty patients (95%) were smokers, with an average SI of 987. The median duration of follow-up was 24 months (range, 1-191 months). Among these, only 23 cases (53%) were definitely diagnosed as having an SCLC

Notes to Table 1
Abbreviations: p, pleural invasion; pm, intrapulmonary metastasis; v, vascular invasion; ly, lymphatic involvement; Adj-CTx, adjuvant chemotherapy; PR, partial response; CTx, chemotherapy; CRTx, chemoradiotherapy; RTx, radiotherapy; Op, Operation; LCC, large cell carcinoma; SD, stable disease; CR, complete response; p/d, poorly differentiated; ca, carcinoma; SQ, squamous cell carcinoma; AD, adenocarcinoma; NSCLC, non–small cell carcinoma, AS, adenosquamous cell carcinoma; NEC, NE carcinoma.
[a] Unknown means that the patient had treatment at another hospital.
[b] Invasion of visceral pleura was graded according to the report of Satoh et al [16]; p1-3 implies that a tumor extends to connective tissues between visceral and parietal pleural membranes.
[c] Double-synchronous primary carcinoma, SQ, and SCLC.
[d] Patients had best supportive care because of poor performance status.
[e] Patients had best supportive care because of his own decision.

Table 2 Immunoreactivity score and serum markers

Cases	Ref. no.	Immunoreactivity score								Serum markers					Group
		NE	SYN	CGA	NCAM	BA	p63	K903	Ki-67 (%)	CEA	SCC	CYFRA	NSE	ProGRP	
1	29635	1	3	3	3	0	1	0	90	3.9	1.1	–	–	–	N+B–
2	30017	1	3	3	3	1	3	0	90	6.4	0.5	–	–	–	N+B+
3	30156	1	3	1	1	1	3	1	100	4	1.1	–	–	–	N+B+
4	30323	1	3	3	3	0	0	0	80	3.1	0.3	–	9.6	–	N+B–
5	30865	1	3	3	3	0	0	0	70	2.3	–	–	–	–	N+B–
6	31160	0	1	0	1	0	0	1	80	7.1	0.5	–	6.7	–	N–B–
7	31401	1	3	0	3	1	1	2	80	4.2	0.7	–	4	–	N+B+
8	32658	1	3	3	3	0	1	1	100	3.9	2.1	–	–	–	N+B–
9	33130	1	3	1	3	0	0	0	60	11.2	–	–	–	–	N+B–
10	33587	1	3	0	3	0	1	0	70	23.9	–	–	–	–	N+B–
11	34802	1	3	1	3	1	3	3	80	4.1	0.9	–	–	–	N+B+
12	34947	1	3	2	3	0	1	0	70	0.8	0.7	–	8.8	–	N+B–
13	35452	1	3	3	3	0	0	1	80	5.5	–	–	4.6	–	N+B–
14	35628	1	3	3	3	0	1	1	100	1.3	4	–	3.2	–	N+B–
15	35996	1	3	3	3	1	2	0	80	1.1	–	–	1.9	–	N+B+
16	36454	1	3	3	3	0	0	0	100	3.2	1.2	–	7.2	–	N+B–
17	36483	1	0	1	3	0	1	0	80	3.2	1.4	–	5.1	–	N+B–
18	36819	1	3	3	3	1	2	0	80	5.4	0.2	–	14.3	–	N+B+
19	38779	1	3	3	3	0	0	1	90	2.1	0.2	–	7.6	70	N+B–
20	38809	1	3	3	3	0	0	0	90	6.7	0.4	–	8.6	–	N+B–
21	39001	1	3	3	3	0	0	1	100	2.3	–	1.3	6.4	29.9	N+B–
22	39080	1	3	3	3	0	1	1	70	8.4	–	–	–	–	N+B–
23	39401	0	0	1	1	0	0	1	90	3.6	2	–	–	–	N–B–
24	39933	0	0	0	1	0	0	1	70	5.7	0.4	4.5	6.7	17.2	N–B–
25	40557	1	3	3	3	1	3	3	100	2.1	0.4	3.5	7.5	20.5	N+B+
26	40805	0	0	0	1	0	0	0	100	3.5	0.7	1.8	6.5	25.5	N–B–
27	40914	1	3	1	3	0	1	0	100	15.1	0.7	2.4	6.6	72.5	N+B–
28	41179	1	3	3	3	0	1	1	70	3.1	1	–	3.8	151	N+B–
29	41310	0	0	1	1	0	1	0	70	6.3	0.3	1.8	4.9	35.3	N–B–
30	42085	0	1	0	0	0	1	1	80	3	0.6	1.3	2.1	20.8	N–B–
31	42253	0	0	1	0	0	0	0	90	5.2	0.4	4.7	13	26.4	N–B–
32	43417	0	1	0	1	0	0	1	90	1.7	–	2.3	10	26.6	N–B–
33	44106	1	3	3	3	0	1	0	100	2.3	0.7	–	–	78.3	N+B–
34	44165	1	3	3	3	0	1	1	90	5.4	1	–	–	–	N+B–
35	44304	1	0	1	2	1	0	3	80	3	0.4	–	–	18.6	N+B+
36	45819	1	3	2	1	0	1	1	100	3.9	–	–	–	49.6	N+B–
37	46287	1	3	3	3	0	0	0	90	5.3	–	–	23	638	N+B–
38	49271	1	3	3	3	0	1	1	100	18.8	0.7	–	6.9	56.2	N+B–
39	50455	1	3	3	3	0	0	0	90	2.6	0.6	–	–	32.4	N+B–
40	40245	0	0	0	0	0	0	0	80	3	0.2	–	12	24.7	N–B–
41	42388	0	0	0	0	0	0	0	70	4.2	–	–	–	–	N–B–
42	44506	1	3	3	3	0	0	0	90	1.9	–	1.2	2.8	16.4	N+B–
43	48003	1	2	3	3	0	0	0	70	0.8	0.9	1.4	–	267	N+B–
Positive ratio (%)		77	72	58	72	19	14	9	70-100	35	10	27	15	40	
N+: positive ratio (%)		100	94	75	94	24	18	12	86.1	33	9	20	11	62	
N–: positive ratio (%)		0	0	0	0	0	0	0	82	40	12	33	25	0	

NOTE. Reference values: CEA, 5.0 ng/mL; SCC, 1.5 ng/mL; CYFRA, 3.5 ng/mL; NSE, 10 ng/mL; ProGRP, 45.9 pg/mL.

before surgery. Most patients received a lobectomy and N2 lymph node dissection, except for 1 segmentectomy for a stage IA case, 1 pneumonectomy for stage IIB, and 2 partial resections. These 2 patients underwent partial resection because one was at a high risk (an advanced age and poor respiratory function) and the other had synchronous double-lung cancer with lobectomy performed for a larger tumor diagnosed as squamous cell carcinoma. Postoperatively, 25

cases were up-staged after identification of N or T factors. All information about the surgical patients is shown in Table 1, including invasion of visceral pleura, as graded for a previous study [16], and prognosis.

The characteristics of the biopsy group (n = 51) were as follows: median age, 67 years (range, 54-85 years); male/female ratio, 44:7; and 96% (43/45) having smoking history (average SI was 1152). One-year and 3-year survival rates were 57% and 2%, respectively. The serum level of ProGRP was higher than the reference value in 49 (96%) of 51 patients, and that of NSE was also higher in 27 (82%) of 33 patients.

Histologic review of resected materials confirmed that all cases were SCLCs according to the WHO classification, including 9 combined types as follows: 4 cases combined with adenocarcinomas, 1 with adenosquamous carcinoma, 1 with spindle cell carcinoma, 2 with large cell carcinoma, and 1 with LCNEC. Atypical cases were reviewed and agreed also by the pathology panel members of the Ministry of Health, Labour and Welfare study group as well as by some of the International Association for the Study of Lung Cancer pathology committee members. Tumors resembling SCLC such as Ewing sarcoma, poorly differentiated synovial sarcoma, lymphoma, squamous cell carcinoma composed of small-sized cells, and BA carcinoma were excluded, based on IHC results and/or close histopathologic observation.

3.3. NE and BA phenotypes in surgical and biopsied cases

Of the surgical patients, 31 (72%) were positive for SYN, 25 (58%) for CGA, 31 (72%) for CD56, 6 (14%) for p63, and 4 (9%) for CK34βE12. Percentages of NE marker positivity (58%-72%) were similar to the previous study based on surgery (57%-58% for SYN and CGA [7]). Immunoreactivity of BA markers might be explained by combined components with SCLC [12], although some cells were positive for both NE and BA markers. Interestingly, there were 8 patients (19%) positive for at least 1 BA marker, and 10 (23%) were negative for all NE markers (Table 2). According to these results, all cases could be classified into 4 subgroups: NE+BA− (n = 25; 58%), NE+BA+ (n = 8; 19%), NE−BA+ (n = 0), and NE−BA− (n = 10; 23%). Histologically, or using the Ki-67 index, it was difficult to distinguish among the 3 groups (Fig. 2; Table 2). When we compared immunoreactivity with several serum markers, the ProGRP value was significantly higher in the NE+ group, and no patients had an abnormal value in the NE− group (P = .023; Table 2), implying a good correlation of the NE phenotype between serum and tumors.

We examined concordance of classification by gene expression profiling and IHC phenotyping. Of 30 SCLC cases analyzed by gene expression profiling, 28 were successfully examined by IHC. All 12 cases classified to group 1 (poor prognosis group) by gene expression profiling fell into the NE+ group by IHC. Of the 16 cases classified to group

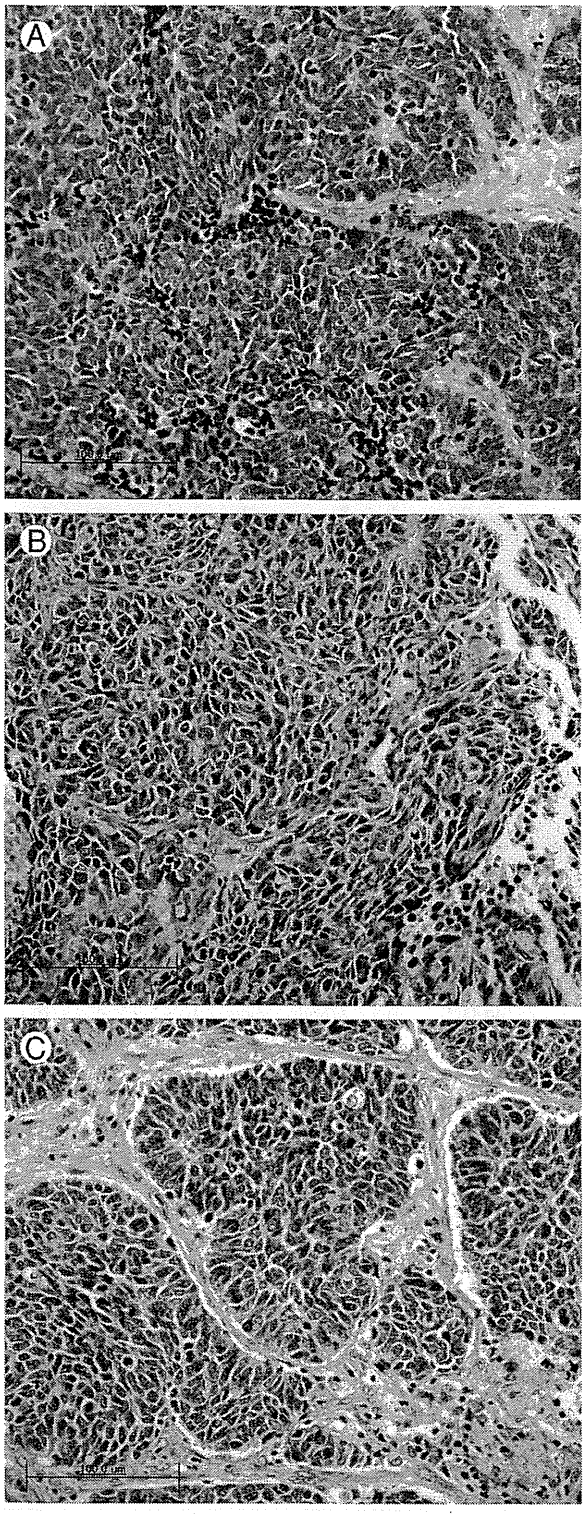

Fig. 2 Representative histologic pictures of SCLC subsets by NE differentiation and BA phenotypes (H&E, original magnification ×40). A, NE+BA−. B, NE+BA+. C, NE−BA−. Notably, there are almost no histopathologic differences among the 3 tumors, including mitosis counts.

Table 3 Comparison of clinicopathological features in the SCLC subgroups with/without NE and BA natures

Variable	No. of cases (n = 43)	NE markers		P	BA markers		P
		Negative (n = 10)	Positive (n = 33)		Negative (n = 35)	Positive (n = 8)	
Age (y)				.481			.7381
<60	10	1	9		9	1	
>61	33	9	24		26	7	
Sex				.718			.8666
Male	34	7	27		27	7	
Female	9	3	6		8	1	
Smoking status				.779			.9287
Never	3	1	2		2	1	
Smoker	40	9	31		33	7	
Tumor size (mm)				.818			.9044
≦30	25	5	20		21	4	
>30	18	5	13		14	4	
Lymph node metastasis				.616			.3605
Negative	25	7	18		22	3	
Positive	18	3	15		13	5	
Pathological stage				.687			.5953
I	17	5	12		15	2	
II-IV	26	5	21		20	6	
Combined subtypes	10	2	8		8	2	
AD	5	1	4		5	0	
SQ	0	0	0		0	0	
AS	1	0	1		0	1	
Spindle	1	0	1		1	0	
LCC	2	0	2		1	1	
LCNEC	1	1	0		1	0	
Induction CTx				.049			.9044
Negative	25	9	16		20	5	
Positive	18	1	17		15	3	
Adjuvant CTx				.56			.9303
Negative	14	2	12		12	2	
Positive	29	8	21		23	6	

Abbreviations: AD, adenocarcinoma; SQ, squamous cell carcinoma; AS, adenosquamous cell carcinoma; LCC, large cell carcinoma; CTx, chemotherapy.
NOTE. All were analyzed by χ^2 test with Yate correction.

2 (good prognosis group), 9 fell in the NE− group and the other 7 in the NE+ group. The concordance rates for groups 1 and 2 were 100% (12/12) and 56% (9/16), respectively.

For biopsy cases, all but 1 were positive for all the 3 NE markers and all were negative for the 2 BA markers. Only 1 patient was negative for CD56 and positive for SYN and CGA. As compared with surgical cases, therefore, the tumors of biopsy cases had a marked NE nature and lacked BA phenotypes.

3.4. Clinicopathological comparison between NE or BA expression and prognosis

We evaluated clinicopathological characteristics according to immunoreactivity for NE and BA markers (Table 3). Unfortunately, only 1 patient in the NE− group underwent induction chemotherapy, so we could not evaluate if the NE− tumors were chemosensitive or not. Rather, this indicated that tumors of the NE− group had almost no influence of chemotherapy and that their characteristics identified by IHC were innate, implying that the results of low NE expression were reliable. No factors showed any significant difference between the BA+ and BA− groups.

SCLC-specific survival curves of NE+/− and BA+/− groups are shown in Fig. 3. There was no difference based on the presence of BA phenotypes (P = .28; Fig. 3A), but NE phenotypes were critical for patient survival. In fact, the NE− group had a significantly better prognosis than did the NE+ group (P = .03; Fig. 3B). Among the 3 groups (NE+BA+, NE+BA−, NE−BA−), the NE−BA− group also showed a significant tendency toward a better outcome (P = .036; Fig. 3C).

3.5. Univariate and multivariate analyses of factors influencing prognosis

Thirty-three surgically treated patients underwent both lobectomy (single or bilobectomy) and platinum-based double chemotherapy (induction and/or adjuvant, ≥4 courses). We used this group with the same treatment condition to evaluate the factors influencing prognosis. Univariate analyses for

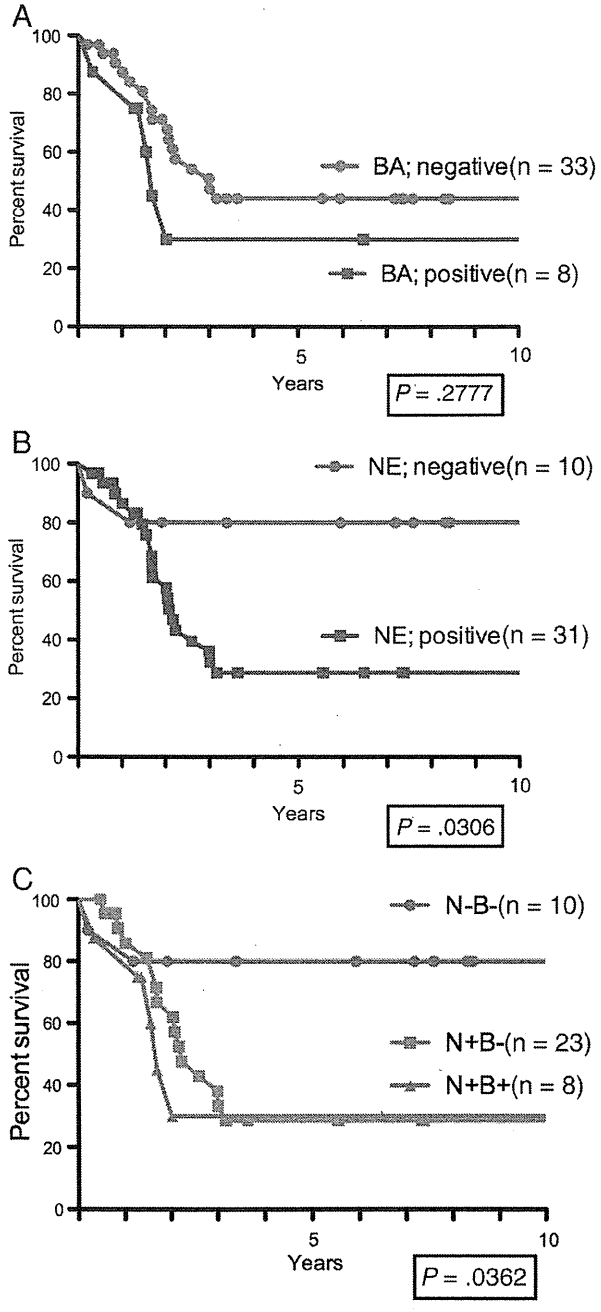

Fig. 3 SCLC-specific survival for patients with or without BA markers (A), $P = .278$, and NE markers (B), $P = .0306$. C, the NE− BA− group features a significantly better prognosis than the others.

overall survival showed that patients negative for NE markers tended to have good prognosis ($P = .047$; Table 4A). When using SCLC-specific survival, univariate analysis showed that both pathological stages ($P = .016$) and NE marker reactivity ($P = .012$) were significant markers for good prognosis. Age, SI, lymphovascular invasion, and BA marker immunoreactivity had no prognostic value. Multivariate analyses revealed that NE marker expression was the only independent factor influencing prognosis (Table 4B; risk ratio, 5.577; 95% confidence interval [CI], 1.172-26.524; $P = .031$). Multivariate analysis for SCLC-specific survival did not produce any significant results probably because the NE− group included no SCLC-specific deaths.

3.6. Induction chemotherapy and its effects on survival

Of the 43 surgical patients analyzed here, 17 (40%) underwent induction chemotherapy, and the reduction rate ranged from 24% to complete response, as detailed in Table 1. Because pretreatment might have some effect on prognosis, we performed survival analyses using 26 cases without pretreatment by comparing SCLC-specific survival between N+ (n = 17) and N− (n = 9) subgroups. As shown in Supplementary Fig. 1A, the survival of NE− subgroup was 3 times better than the NE+ subgroup. Although the difference was not significant ($P = .148$), this was probably due to the small number of cases. Furthermore, we compared SCLC death rates and survival difference of NE+ cases (n = 33) between those with induction chemotherapy (n = 16) and without (n = 17). They were 11 (69%) of 16 for cases with the pretreatment and 9 (53%) of 17 for cases without and were not significantly different. Also, as Supplementary Fig. 1B indicates, survival was not different between the 2 subgroups ($P = .19$), although the number of cases was larger than the analysis using non-pretreated cases. Based on these findings, we used all the cases including cases both with and without pretreatments for survival analysis.

4. Discussion

To our knowledge, this is the first report describing a hitherto unmarked SCLC subtype with a good prognosis, using substantial numbers of surgically resected cases. Here we demonstrated that the subtype can be detected by IHC alone using NE markers such as SYP, CGA and CD56. Previously, we identified the subtype by global gene expression profiling using cDNA microarrays. The current study, using oligonucleotide arrays (by Affymetrix), duplicated fairly well the subset with additional new cases. Also in this study, we focused on characterizing the SCLC subset by hypothesizing that low expression of NE-related proteins and/or a BA nature of tumor cells might explain differences from standard SCLCs.

In fact, BA carcinoma histologically resembles SCLC, and the BA pattern is a marker for worse prognosis for non-SCLC [17]. Our univariate and multivariate analyses reveal, however, that expression of NE markers is a prognostic factor, but the BA phenotype in terms of CK34βE12 and p63 protein expression has no effect on survival. The immunohistochemically defined obvious subtype of SCLC with a good prognosis comprised 23% of the surgically resected SCLC. Because there were no such cases in

Table 4 Univariate and multivariate analyses on factors influencing overall survival, based on all cases (n=96, surgery [n=45] and biopsy [n=51]). (A) analyses for SCLC-specific survival (B)

Parameters	A					B
	Univariate	Multivariate				Univariate
	P	*P*	Exp (coefficient)	Lower (95% CI)	Upper (95% CI)	*P*
Age (>60 y)	.900	.666	1.256	0.447	3.525	.618
Sex	.777					.303
Pathological stage (>I)	.135	.095	2.381	0.860	6.592	.016
Vascular invasion	.886					.174
Lymphatic invasion	.827					.534
NE marker	.047	.031	5.577	1.172	26.524	.012
BA marker	.777	.331	0.559	0.173	1.804	.208

inoperable patients, we could not perform a study using only biopsy materials.

According to the current WHO criteria for NE tumors, it is necessary to prove NE phenotypes for LCNEC diagnosis, but not for SCLCs. In the present study, approximately 80% of surgical tumors had NE phenotypes, largely consistent with the previous studies [7,18,20], and all the biopsy cases had obvious NE phenotypes proven by IHC. Although this fact suggests that the current WHO criteria work quite well, they are insufficient to distinguish the atypical SCLC subtype with a good prognosis, particularly for surgical cases.

Serum tumor markers including NSE, ProGRP, and CD56 are useful for clinical diagnosis of SCLC, and their immunohistochemical staining has been used for discrimination of NE tumors from others. However, their prognostic value has proved controversial [21,23]. In this study, we demonstrated immunohistochemical use for outcome prediction. Also, the NE marker levels in serum tended to be higher in the group with a poor prognosis. In fact, almost all the cases with elevated serum markers belonged to the poor prognosis group, as shown in Table 2. Because the number of cases with measured serum NE markers in the good prognosis group is limited, we should continue comparing the prognosis between groups with and without elevated values.

Chemosensitivity and radiosensitivity is crucial for SCLC treatment. Unfortunately, we were unable to determine if our NE− (negative) group was chemosensitive or not because none of the cases underwent induction chemotherapy or treatment of a recurrent tumor. We should further investigate sensitivity by accumulating more cases of this particular SCLC subtype.

Although it is difficult to distinguish histologically an SCLC subtype with a good prognosis, such a subtype may exist, which has distinct cellular and genetic characteristics. In our previous study [13], we performed an integrated analysis using clinical SCLC tumors and established SCLC cell lines. As a matter of fact, there were no cell lines that clustered together with the good prognosis subtype. Therefore, further studies may include establishing cell lines of this particular SCLC subtype.

Supplementary data

Supplementary data to this article can be found online at http://dx.doi.org/10.1016/j.humpath.2014.01.001.

Acknowledgments

The authors thank Dr E. Miyauchi, Mr Satoshi Miyata, Mr Motoyoshi Iwakoshi, Ms Tomoyo Kakita, Ms Mayumi Ogawa, and Ms Keiko Shiozawa for their statistical and technical assistance and Ms Yuki Takano and Ms Hiroko Nagano for their secretarial expertise. Also, the authors thank Dr Michael H. Jones for his expert English editing.

References

[1] Karnofsky DA, Abelmann WH, Craver LF. The use of the nitrogen mustards in the palliative treatment of carcinoma. Cancer 1948:634-56.
[2] Miller AB, Fox W, Tall R. Five-year follow-up of the medical research council comparative trial of surgery and radiotherapy for the primary treatment of small-celled or oat-celled carcinoma of the bronchus. the Lancet 1969;2:501-5.
[3] Green RA, Humphrey E, Close H, Patno ME. Alkylating agents in bronchogenic carcinoma. Am J Med 1969;46:516-25.
[4] Pujol JL, Carestia L, Daures JP. Is there a case for cisplatin in the treatment of small-cell lung cancer? A meta-analysis of randomized trials of a cisplatin-containing regimen versus a regimen without this alkylating agent. Br J Cancer 2000;83:8-15.
[5] Pignon JP, Arriagada R, Ihde DC, et al. A meta-analysis of thoracic radiotherapy for small-cell lung cancer. N Engl J Med 1992;327:1618-24.
[6] Elias AD. Small cell lung cancer: state-of-the-art therapy in 1996. Chest 1997;112:251S-8S.
[7] Nicholson SA, Beasley MB, Brambilla E, et al. Small cell lung carcinoma (SCLC): a clinicopathologic study of 100 cases with surgical specimens. Am J Surg Pathol 2002;26:1184-97.
[8] Tsuchiya R, Suzuki K, Ichinose Y, et al. Phase II trial of postoperative adjuvant cisplatin and etoposide in patients with completely resected stage I-IIIa small cell lung cancer: the Japan Clinical Oncology Lung Cancer Study Group Trial (JCOG9101). J Thorac Cardiovasc Surg 2005;129:977-83.
[9] Asamura H, Kameya T, Matsuno Y, et al. Neuroendocrine neoplasms of the lung: a prognostic spectrum. J Clin Oncol 2006;24:70-6.

[10] Travis WD, Brambilla E, Muller-Hermelink HK, et al. Pathology and genetics of tumours of the lung, pleura, thymus and heart. World Health Organization Classification of Tumours. Lyon: IACR Press; 2004.
[11] Viberti L, Bongiovanni M, Croce S, Bussolati G. 34betaE12 cytokeratin—immunodetection in the differential diagnosis of small cell tumors of lung. Int J Surg Pathol 2000;8:317-22.
[12] Sturm N, Lantuejoul S, Laverriere MH, et al. Thyroid transcription factor 1 and cytokeratins 1, 5, 10, 14 (34betaE12) expression in basaloid and large-cell neuroendocrine carcinomas of the lung. Hum Pathol 2001;32:918-25.
[13] Jones MH, Virtanen C, Honjoh D, et al. Two prognostically significant subtypes of high-grade lung neuroendocrine tumours independent of small-cell and large-cell neuroendocrine carcinomas identified by gene expression profiles. Lancet 2004;363:775-81.
[14] Sobin H, Wittekind C, editors. TNM classification of malignant tumours. 5th ed. Geneva: UICC; 1997.
[15] Irizarry RA, Hobbs B, Collin F, et al. Exploration, normalization, and summaries of high density oligonucleotide array probe level data. Biostatistics 2003;4:249-64.
[16] Satoh Y, Ishikawa Y, Inamura K, Okumura S, Nakagawa K, Tsuchiya E. Classification of parietal pleural invasion at adhesion sites with surgical specimens of lung cancer and implications for prognosis. Virchows Arch 2005;447:984-9.
[17] Moro-Sibilot D, Lantuejoul S, Diab S, et al. Lung carcinomas with a basaloid pattern: a study of 90 cases focusing on their poor prognosis. Eur Respir J 2008;31:854-9.
[18] Miyahara R, Tanaka F, Nakagawa T, Matsuoka K, Isii K, Wada H. Expression of neural cell adhesion molecules (polysialylated form of neural cell adhesion molecule and L1-cell adhesion molecule) on resected small cell lung cancer specimens: in relation to proliferation state. J Surg Oncol 2001;77:49-54.
[19] Travis WD. Update on small cell carcinoma and its differentiation from squamous cell carcinoma and other non-small cell carcinomas. Mod Pathol 2012;25(Suppl 1):S18-30.
[20] Hiroshima K, Iyoda A, Shida T, et al. Distinction of pulmonary large cell neuroendocrine carcinoma from small cell lung carcinoma: a morphological, immunohistochemical, and molecular analysis. Mod Pathol 2006;19:1358-68.
[21] Pujol JL, Quantin X, Jacot W, Boher JM, Grenier J, Lamy PJ. Neuroendocrine and cytokeratin serum markers as prognostic determinants of small cell lung cancer. Lung Cancer 2003;39:131-8.
[22] Jaques G, Auerbach B, Pritsch M, Wolf M, Madry N, Havemann K. Evaluation of serum neural cell adhesion molecule as a new tumor marker in small cell lung cancer. Cancer 1993;72:418-25.
[23] Lamy PJ, Grenier J, Kramar A, Pujol JL. Pro-gastrin–releasing peptide, neuron specific enolase and chromogranin A as serum markers of small cell lung cancer. Lung Cancer 2000;29:197-203.

Oncogene (2013) **32,** 2140–2149

www.nature.com/onc

ORIGINAL ARTICLE

FHL1 on chromosome X is a single-hit gastrointestinal tumor-suppressor gene and contributes to the formation of an epigenetic field defect

K Asada[1,7], T Ando[1,2,7], T Niwa[1], S Nanjo[1], N Watanabe[1], E Okochi-Takada[1], T Yoshida[1], K Miyamoto[3], S Enomoto[4], M Ichinose[4], T Tsukamoto[5], S Ito[6], M Tatematsu[5], T Sugiyama[2] and T Ushijima[1]

Tumor-suppressor genes on chromosome X can be inactivated by a single hit, any of the point mutations, chromosomal loss and aberrant DNA methylation. As aberrant DNA methylation can be induced frequently, we here aimed to identify a tumor-suppressor gene on chromosome X inactivated by promoter DNA methylation. Of 69 genes on chromosome X upregulated by treatment of a gastric cancer cell line with a DNA-demethylating agent, 5-aza-2′-deoxycytidine, 11 genes had low or no expression in the cell line and abundant expression in normal gastric mucosae. Among them, *FHL1* was frequently methylation-silenced in gastric and colon cancer cell lines, and methylated in primary gastric (21/80) and colon (5/50) cancers. Knockdown of the endogenous *FHL1* in two cell lines by two kinds of shRNAs significantly increased cell growth *in vitro* and sizes of xenografts in nude mice. Expression of exogenous *FHL1* in a non-expressing cell line significantly reduced its migration, invasion and growth. Notably, a somatic mutation (G642T; Lys214Asn) was identified in one of 144 colon cancer specimens, and the mutant *FHL1* was shown to lack its inhibitory effects on migration, invasion and growth. *FHL1* methylation was associated with *Helicobacter pylori* infection and accumulated in normal-appearing gastric mucosae of gastric cancer patients. These data showed that *FHL1* is a methylation-silenced tumor-suppressor gene on chromosome X in gastrointestinal cancers, and that its silencing contributes to the formation of an epigenetic field for cancerization.

Oncogene (2013) **32,** 2140–2149; doi:10.1038/onc.2012.228; published online 11 June 2012

Keywords: field for cancerization; chromosome X; DNA methylation; gastrointestinal cancer; *Helicobacter pylori*

INTRODUCTION

Inactivation of tumor-suppressor genes is deeply involved in cancer development and progression.[1] The vast majority of tumor-suppressor genes are somatically inactivated by two hits of both alleles by genetic and/or epigenetic mechanisms, such as point mutations, chromosomal deletions and aberrant DNA methylation of promoter CpG islands (CGIs).[2,3] The two-hit theory makes tumor-suppressor genes on chromosome X unique because they can be inactivated by a single hit, and thus are 'risky' genes. So far, three examples have been identified, including *WTX* in Wilms tumors,[4] *FOXP3* in breast and prostate cancers[5,6] and *PHF6* in T-cell acute lymphoblastic leukemia (T-ALL),[7] all of which are inactivated by a point mutation or chromosomal loss.

Among the mechanisms of tumor-suppressor gene inactivation, aberrant DNA methylation can be present not only in tumor tissues but also in normal-appearing tissues, such as non-cancerous tissues of gastric,[8,9] colon,[10] liver,[11] esophageal,[12–14] breast[15] and renal cancer patients.[16] Levels of aberrant DNA methylation in non-cancerous tissues correlate with cancer risk clearly for gastric cancers[8,17] and other cancers, and accumulation of aberrant DNA methylation in a tissue is considered to form an epigenetic field for cancerization (epigenetic field defect).[18] Such association has been analyzed using methylation levels of marker genes, which are methylated in association with various tumor-suppressor genes and show much higher levels, and only a limited number of genes that functionally contribute to the field defect have been identified.

To identify risky genes that contribute to the formation of an epigenetic field defect, we here searched for genes on chromosome X from the 495 genes whose expression was upregulated fourfold or more after treatment with a DNA-demethylating agent, 5-aza-2′-deoxycytidine (5-aza-dC)[19] of a gastric cancer cell line (AGS), which is known to have very frequent methylation of CGIs.[20]

RESULTS

Screening of methylation-silenced genes on chromosome X

Among the 495 genes whose expression was upregulated fourfold or more by treatment of the AGS gastric cancer cell line with 5-aza-dC, 69 genes were located on chromosome X. Among the 69 genes, 11 genes had low expression (signal intensity <200) in non-treated AGS cells and had high expression (signal intensity >500) in a pool of gastric mucosae of three healthy volunteers.

[1]Division of Epigenomics, National Cancer Center Research Institute, Tokyo, Japan; [2]Third Department of Internal Medicine, University of Toyama, Toyama, Japan; [3]Institute for Clinical Research and Department of Surgery, National Hospital Organization Kure Medical Center/Chugoku Cancer Center, Hiroshima, Japan; [4]Second Department of Internal Medicine, Wakayama Medical University, Wakayama, Japan; [5]Division of Oncological Pathology, Aichi Cancer Center Research Institute, Nagoya, Japan and [6]Department of Gastroenterological Surgery, Aichi Cancer Center Hospital, Nagoya, Japan. Correspondence: Dr T Ushijima, Division of Epigenomics, National Cancer Center Research Institute, 5-1-1 Tsukiji, Chuo-ku, Tokyo 104-0045, Japan.
E-mail: tushijim@ncc.go.jp
[7]These authors contributed equally to this work.
Received 20 September 2011; revised 25 April 2012; accepted 4 May 2012; published online 11 June 2012

Genomic structures were analyzed for these 11 genes, and eight of them had CGIs in their promoter regions (Supplementary Table 1). Their mRNA expression levels were confirmed by quantitative reverse transcription–PCR (qRT–PCR) in non-treated AGS cells and gastric epithelial cells obtained by the gland isolation technique, and five (*MAOA, CXorf26, FHL1, SMARCA1* and *MAOB*) had consistent expression in gastric epithelial cells (Supplementary Table 1). Among the five genes, we focused on the *FHL1* gene, because it was reported to be able to inhibit growth, migration, invasion and metastasis of multiple types of cancer cells.[21–26] The other four genes were not reported to be involved in cancer development in the literature.

Promoter methylation and silencing of *FHL1* in gastrointestinal cancer cell lines

DNA methylation status of the *FHL1* promoter region was analyzed using two sets of methylation-specific PCR (MSP) primers designed to cover a region from the transcription start site to 220 bp upstream (Figure 1a). Among the 73 cancer cell lines analyzed (11 gastric, 7 colon, 12 lung, 12 skin, 7 pancreas, 4 esophageal, 4 prostate, 6 breast and 10 ovary cancer cell lines; Supplementary Table 2), *FHL1* was completely methylated (no unmethylated DNA molecules detected) in seven gastric, three colon (Figure 1b) and one lung cancer cell lines. In normal-appearing gastric and colonic mucosae, and peripheral leukocytes of healthy volunteers, *FHL1* was completely unmethylated in males, and partially methylated in females (Figure 1c). The partial methylation in females was considered to reflect methylation of the inactive chromosome X, which is shown later.

The role of the promoter methylation in downregulation of *FHL1* expression was analyzed. First, an association between the methylation and loss of expression was confirmed among the 11 gastric and 7 colon cancer cell lines. *FHL1* was consistently unexpressed in seven gastric and three colon cancer cell lines with its complete methylation (Figures 2a and b), but was expressed in most of the cancer cell lines without methylation, in normal colonic epithelial cells (CRL1790 and CRL1831) and in normal-appearing gastric and colonic mucosae. Second, when promoter methylation was removed by 5-aza-dC treatment of AGS and

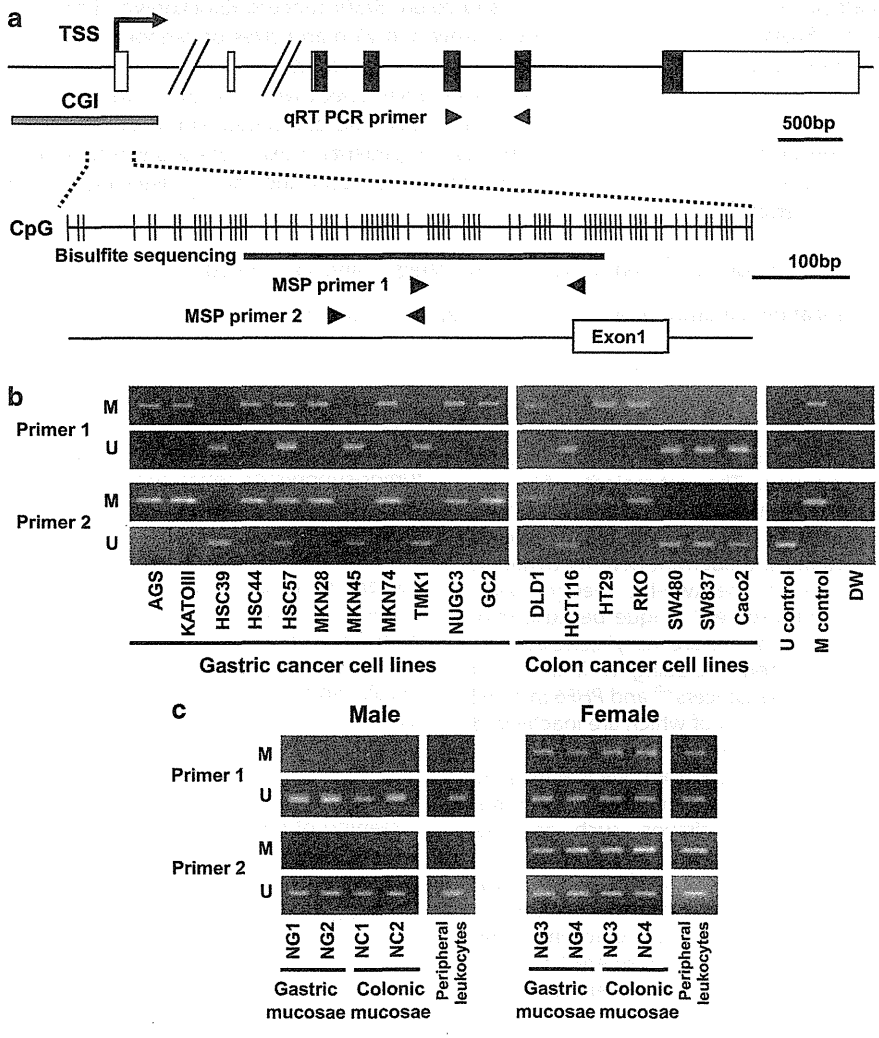

Figure 1. Genomic structure of *FHL1* and its methylation status in cancer cell lines, normal-appearing mucosae and peripheral leukocytes. (**a**) Genomic structure of *FHL1* and a CpG map of its promoter CGI. Open box, non-coding exon; closed box, coding exon; arrow, transcription start site (TSS); gray box, CGI region; vertical lines, individual CpG sites; arrowheads, primers for qRT–PCR and MSP; and bold line and number, the region and individual CpG sites analyzed by bisulfite sequencing. (**b**) Promoter methylation of *FHL1* in 11 gastric and seven colon cancer cell lines analyzed by MSP. M and U, primer sets specific to methylated and unmethylated DNA, respectively; U control, fully unmethylated genomic DNA; and M control, fully methylated genomic DNA. *FHL1* was frequently methylated in gastric and colon cancer cell lines. (**c**) Promoter methylation of *FHL1* in male and female normal-appearing gastric and colonic mucosae and peripheral leukocytes. *FHL1* was completely unmethylated in males and partially methylated in females.

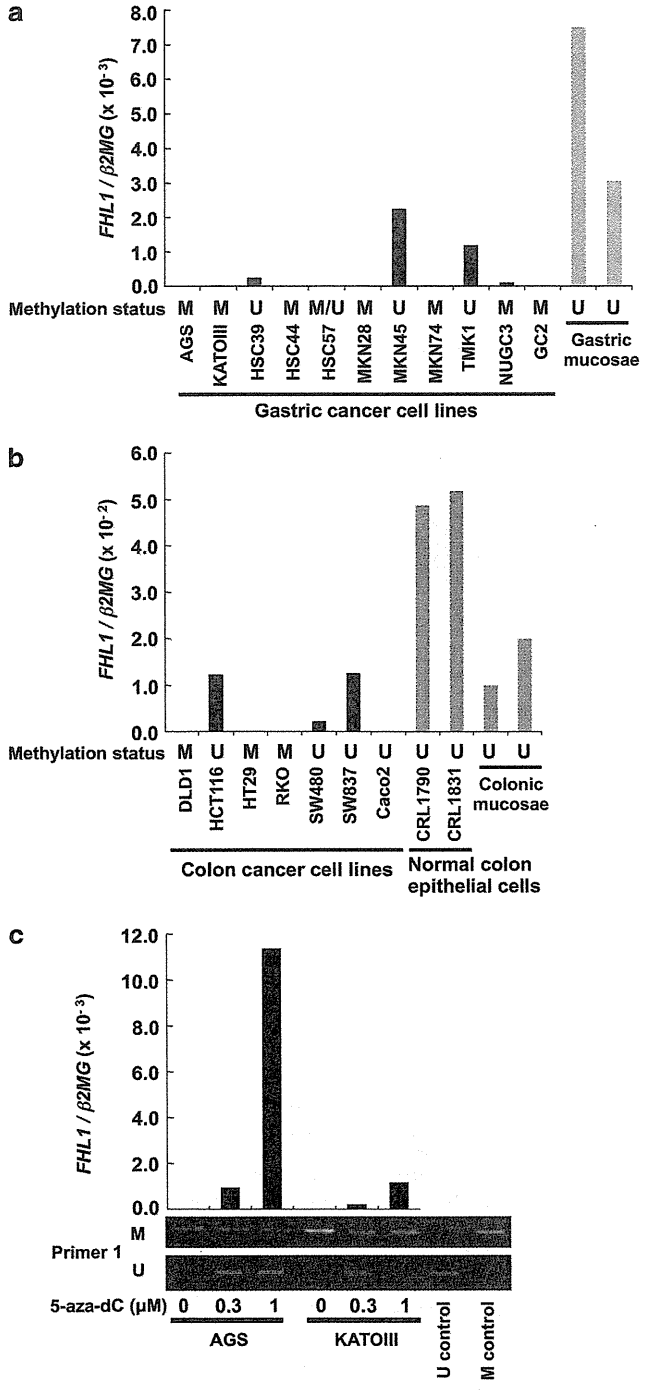

Figure 2. Methylation-silencing of *FHL1* in gastrointestinal cancer cell lines. (**a**) qRT–PCR of *FHL1* in gastric cancer cell lines and normal-appearing gastric mucosae. Results of MSP in Figure 1b are shown by M, M/U and U. M, only methylated DNA detected; M/U, both methylated and unmethylated DNA detected; and U, only unmethylated DNA detected. *FHL1* was not expressed in cell lines with complete methylation. (**b**) qRT–PCR of *FHL1* in colon cancer cell lines, normal colonic epithelial cells and normal-appearing colonic mucosae. *FHL1* was not expressed in cell lines with complete methylation. (**c**) Re-expression and demethylation of *FHL1* after 5-aza-dC treatment of AGS and KATOIII. *FHL1* expression was induced, along with its demethylation, after treatment with 5-aza-dC. U control, fully unmethylated genomic DNA; and M control, fully methylated genomic DNA.

KATOIII gastric cancer cell lines, *FHL1* expression was restored (Figure 2c). These data demonstrated that promoter methylation of *FHL1* caused its silencing.

Methylation of *FHL1* in surgical gastrointestinal cancer specimens

FHL1 methylation in surgical cancer specimens was analyzed by quantitative real-time MSP (qMSP) of 80 gastric and 50 colon cancers derived from male patients (Figure 3a). We adopted a cutoff value of 6%, which was previously determined based on the lowest methylation levels of tumor-suppressor genes in cancer samples,[9,27] and was also used in other researchers' report.[28] *FHL1* was methylated in 21 of the 80 (26%) gastric cancers and 5 of the 50 (10%) colon cancers. The presence of dense methylation of the promoter region was confirmed by bisulfite sequencing, and the fraction of densely methylated DNA molecules was in accordance with the methylation level obtained by qMSP (Figure 3b).

Association between promoter methylation and decreased expression was analyzed in 33 cancer specimens for which RNA was available. The mean *FHL1* expression level of 11 cancers with methylation was significantly lower than that of 22 cancers without methylation ($P=0.04$) (Figure 3c). Considering that surgical cancer specimens are contaminated with normal cells, the findings here supported that *FHL1* was methylation-silenced also in surgical cancer specimens.

Association between *FHL1* methylation and the CpG island methylator phenotype

Clinicopathological characteristics of cancers with *FHL1* methylation were analyzed in the 80 gastric cancers. *FHL1* methylation was not associated with tumor invasion, lymph node metastasis and histological type (Table 1). In contrast, *FHL1* methylation was associated with the presence of the CGI methylator phenotype (CIMP), 17 of 21 cancers with *FHL1* methylation (81%) and 13 of 59 without being CIMP-positive (22%; $P=2.9\times10^{-6}$). *FHL1* methylation was associated with the presence of Epstein–Barr virus (EBV) infection ($P=0.02$), but not with *hMLH1* methylation. This suggested that, between the two subtypes of CIMP-positive gastric cancers (those with EBV infection and those with *hMLH1* methylation),[29] *FLH1* methylation was associated with the former.

Growth-suppressive activity of *FHL1*

The effect of the *FHL1* expression loss on cell growth was analyzed by knocking down *FHL1* first *in vitro*. Two *FHL1*-specific shRNAs (sh1and sh2), along with a control shRNA (luciferase-specific shRNA; Luc-sh), were introduced into two cancer cell lines with *FHL1* expression (HCT116 and HSC39). *FHL1* expression was confirmed to be strongly suppressed by sh1 (11.7% of the control cells) and sh2 (14.8%) by qRT–PCR and also by western blot (Figure 4a). *FHL1* knockdown accelerated cell growth in HCT116 cells (sh1, 243% of control cells at 120 h, $P<0.001$, and sh2, 191%, $P<0.001$) and in HSC39 cells (sh1, 144% of control cells at 96 h, $P<0.01$, and sh2, 130%, $P<0.01$) (Supplementary Figure 1). Then, *in vivo* growth assay using a nude mouse xenograft model showed that HCT116 cells with *FHL1* knockdown formed 2.7-fold larger tumors than control cells (Luc-sh) ($P<0.001$) (Figure 4b), and that their mean weight was 2.8-fold heavier than that of control cells (Figure 4c). The maintenance of *FHL1* decrease by shRNA was confirmed (Supplementary Figure 2).

The growth-suppressive activity was further analyzed by expressing exogenous *FHL1* in two non-expressing cell lines (AGS and MKN28). By qRT–PCR and western blot, expression levels of the exogenous *FHL1* in AGS and MKN28 were shown to be ~10-and 40-fold, respectively, of those in non-cancerous gastric mucosae (Figures 4d and 5a, and Supplementary Figure 3a). *FHL1* expression reduced the cell growth in AGS (72.2% of control

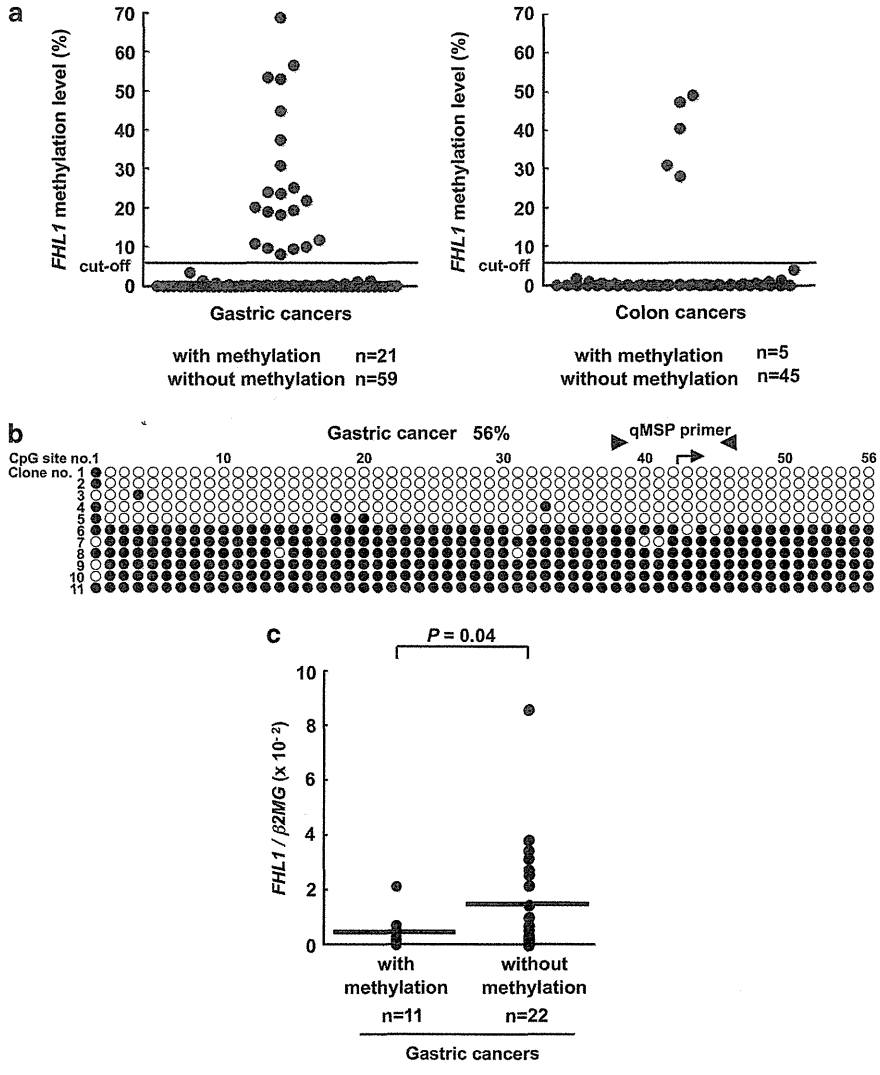

Figure 3. Methylation of *FHL1* in surgical gastrointestinal cancer specimens and its effect on expression. (**a**) Methylation levels in gastric (left) and colon (right) cancers derived from male patients. A horizontal line shows a cutoff value of 6%. *FHL1* was methylated in 21 of 80 primary gastric cancers and 5 of 50 colon cancers, respectively. (**b**) Confirmation of *FHL1* methylation by bisulfite sequencing. Fifty-six CpG sites were analyzed in a gastric cancer with a methylation level of 56%, and six of 11 DNA molecules were densely methylated. Closed circle, methylated CpG site; open circle, unmethylated CpG site; arrowheads, primers for qMSP; and arrow, transcription start site. (**c**) Decreased expression of *FHL1* in gastric cancers with methylation analyzed by qRT–PCR. A horizontal line represents the mean expression level in each group.

cells at 120 h, $P<0.05$; Figures 4d and 5b) but not in MKN28 (Supplementary Figure 3b).

Inhibitory effects of *FHL1* on migration and invasion

To clarify the mechanisms of how *FHL1* works as a tumor-suppressor gene, inhibitory effects of *FHL1* on cell migration and invasion were analyzed in two cell lines (AGS and MKN28). *FHL1* inhibited cell migration both in AGS (26.6% of control cells, $P<0.01$, Figure 5c) and in MKN28 (33.1% of control cells, $P<0.01$, Supplementary Figure 3c). In addition, *FHL1* inhibited cell invasion both in AGS ($P<0.05$, Figure 5d) and in MKN28 ($P<0.05$, Supplementary Figure 3d). In contrast, no induction of apoptosis was observed in AGS by terminal deoxynucleotidyl transferase dUTP nick end labeling assay (Supplementary Figure 4).

An *FHL1* mutation and its loss of function

FHL1 mutations were analyzed by sequencing its seven exons in 58 gastric and 144 colon cancer specimens derived from male patients. A somatic mutation (G642T; Lys214Asn) in exon 6 was identified in a colon cancer (Figure 5e). Also, a synonymous polymorphism (C450T) was observed in two gastric cancers. In the cancer with the G642T mutation, *FHL1* methylation was absent (data not shown), suggesting that either this mutation or promoter methylation was sufficient to inactivate *FHL1*. Further, the effects of the G642T mutation were analyzed by exogenously expressing the mutant and wild-type *FHL1* at similar levels (Figure 5a and Supplementary Figure 3a) in non-expressing AGS and MKN28 cells. The mutant *FHL1* lacked the inhibitory effects on migration and invasion both in AGS (Figures 5c and d) and in MKN28 (Supplementary Figures 3c and d). The mutant *FHL1* also lacked its inhibitory effect on cell growth in AGS (Figure 5b), whereas such effect could not be analyzed in MKN28, whose growth was not suppressed even by wild-type *FHL1*. These data indicated that the mutation was a loss-of-function mutation.

FHL1 methylation levels in non-cancerous gastric and colonic mucosae

To analyze the association between *FHL1* methylation and *Helicobacter pylori* (*H. pylori*) infection, and the contribution of

Table 1. Association between clinicopathological characteristics of patients and *FHL1* promoter methylation

Characteristics	*FLH1 methylation*		P
	Positive (N = 21)	*Negative (N = 59)*	
Tumor invasion			
≤T2	13	33	0.80
>T2	8	26	
Lymph node metastasis			
Positive	15	50	0.20
Negative	6	9	
Histological type			
Intestinal	8	27	0.61
Diffuse	13	32	
CIMP			
Positive	17	13	2.9×10^{-6}
Negative	4	46	
EBV infection			
Positive	4	1	0.02
Negative	17	58	
hMLH1 *methylation*			
Positive	4	5	0.23
Negative	17	54	

Abbreviations: CIMP, CGI methylator phenotype; EBV, Epstein–Barr virus.

FHL1 methylation to the formation of an epigenetic field defect, *FHL1* methylation levels were quantified in gastric mucosae of male healthy volunteers (with and without *H. pylori* infection; 16 each) and non-cancerous mucosae of male gastric cancer patients (with and without *H. pylori* infection; 26 each) (Figure 6a). Among the healthy volunteers, *FHL1* methylation was elevated only in *H. pylori*-positive individuals (10 of 16, 62.5%; $P = 0.01$, *t*-test). As potent methylation induction by *H. pylori* can mask a difference in *H. pylori*-positive individuals,[8] *FHL1* methylation levels were compared between healthy volunteers and gastric cancer patients among the *H. pylori*-negative individuals. *FHL1* methylation level was shown to be elevated only in gastric cancer patients (5 of 26, 19.2%; $P = 0.09$, *t*-test). In the case of the colon, *FHL1* methylation was elevated in colonic mucosae of only 2 of 50 colon cancer patients (4%) (Supplementary Figure 5).

FHL1 methylation levels in female specimens

FHL1 methylation levels were analyzed in female specimens, including gastric mucosae of healthy volunteers (18 with *H. pylori* infection and 10 without), those of gastric cancer patients (7 with *H. pylori* infection and 11 without) and one specimen of peripheral leukocytes (Figure 6b). As in male specimens, among the healthy volunteers, *FHL1* methylation levels were significantly elevated in *H. pylori*-positive individuals ($P = 0.01$, *t*-test). Among the *H. pylori*-negative individuals, they tended to be higher in cancer patients than those in healthy volunteers ($P = 0.06$, *t*-test). *FHL1* methylation levels in *H. pylori*-negative female specimens were expected to be 50% because *FHL1* is located on chromosome X, but its actual distribution was between 20 and 40%. Bisulfite sequencing of the *FHL1* promoter region showed that female specimens contained DNA molecules with sparse methylation of CpG sites (Figure 6c), which was in contrast with the dense methylation in cancer specimens (Figure 3b). It was considered that the inactive chromosome X had sparse methylation of the *FHL1* promoter region not detected by qMSP.

DISCUSSION

The *FHL1* gene on chromosome X was shown to be a tumor-suppressor gene in gastrointestinal cancers by the presence of its methylation-silencing, its inhibitory effects on migration, invasion and growth, and the presence of a loss-of-function mutation. Notably, a loss-of-function mutation was identified for the first time in any type of cancers. This added *FHL1* as a new member of 'risky' tumor-suppressor genes on chromosome X, and the first tumor-suppressor gene on chromosome X that can be inactivated by methylation-silencing. *FHL1* methylation was associated with *H. pylori* infection and strongly accumulated in gastric mucosae of gastric cancer patients. Together with the fact that *FHL1* is a tumor-suppressor gene, the accumulation of *FHL1* methylation was considered to contribute to the formation of a field for cancerization as a driver.

Downregulation of *FHL1* in surgical specimens has been reported in breast, renal, prostate,[23] gastric,[25] liver,[21] and lung cancers.[22] The downregulation was associated with short patient survival and deep invasion in gastric cancers,[25] and with poor differentiation in lung cancers.[22] As a mechanism for the downregulation, methylation silencing was described in bladder cancers.[24] Functionally, *FHL1* has been reported to suppress growth of lung, liver and breast cancer cells and transformed fibroblasts,[21,22,26,30] and migration and invasion of bladder cancer cells and transformed fibroblasts.[24,26] The data obtained here were in line with previous reports, and demonstrated that *FHL1* inhibits migration and invasion in gastrointestinal cancer cells.[22]

Mechanistically, FHL1 is characterized by the presence of four and a half highly conserved LIM domains, which are involved in a wide range of protein–protein interactions, including actin cytoskeleton, cellular signaling proteins and transcriptional machinery.[31] In hepatocellular carcinomas, FHL1 was shown to interact with Smad2 and activate TGF-β pathway independently of TGF-β.[21] In breast cancers, FHL1 was shown to interact with estrogen receptor-α and estrogen receptor-β, and repress estrogen-responsive gene transcription.[30] Proteins that interact with FHL1 in gastric and colonic epithelial cells have not been clarified yet. However, inactivation of the TGF-β pathway is known to be involved in these cancers,[32] and is a strong candidate mechanism of how *FHL1* inactivation is involved in these gastrointestinal cancers.

FHL1 methylation was present not only in cancer tissues, but also in non-cancerous gastric mucosae of gastric cancer patients (5 of 26) and in non-cancerous colonic mucosae of colon cancer patients (2 of 50). This showed, for the first time in any types of cancers, that *FHL1* methylation silencing is involved in the formation of the epigenetic field defect as a driver. So far, only a limited number of driver genes, including *CDKN2A*, *CDH1* and *LOX*, are known to be involved in the formation of an epigenetic field defect.[18] For those genes on autosomes, it is difficult to estimate what fraction of cells has biallelic methylation. In contrast, in the case of *FHL1*, its methylation level linearly correlates with the fraction of cells with its inactivation, and, even if its methylation level is low, the presence of its methylation is expected to bring a significant impact. *H. pylori* infection is known to induce aberrant methylation that consists of temporary and permanent components,[8,33] and the high methylation levels in individuals with current *H. pylori* infection were in accordance with this previous finding.

In females, approximately half of the DNA molecules were methylated, densely or sparsely, in gastric mucosae and peripheral leukocytes of healthy volunteers without *H. pylori* infection by bisulfite sequencing. As no methylated DNA molecules were detected in a male specimen, both the densely and sparsely methylated DNA molecules in female specimens were considered to be derived from the inactive X allele.[34] However, we were not able to demonstrate it because a polymorphism that can

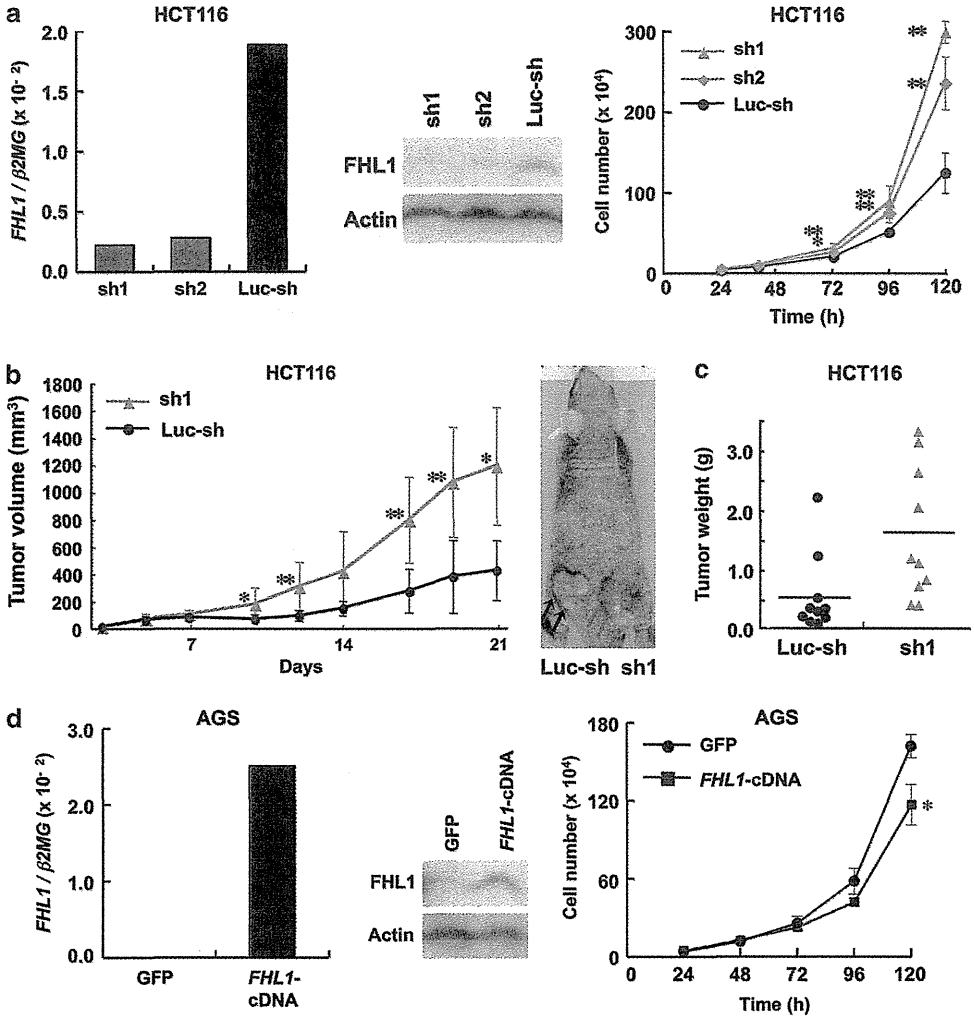

Figure 4. Growth-suppressive activity of *FHL1 in vitro* and *in vivo*. (**a**) *FHL1* knockdown and the resultant increased growth of HCT116 cells. Decreased expression of *FHL1* by its knockdown was confirmed by qRT–PCR (left) and western blot (middle). Growth rates of cells with *FHL1* knockdown were shown to be increased (*$P<0.01$, **$P<0.001$) (right). Data are shown as the mean of three independents ± s.d. (**b**) Increased *in vivo* growth of HCT116 cells with *FHL1* knockdown. Cells with *FHL1* knockdown (sh1) showed a 2.7-fold larger tumor volume compared with the control cells (Luc-sh) (*$P<0.01$, **$P<0.001$). Data are shown as the mean ± s.d. Arrows, tumors produced. (**c**) Increased tumor weight of cells with *FHL1* knockdown (sh1). Mean tumor weight of cells with knockdown (sh1) ($n=10$) was 2.8-fold heavier than that of controls (Luc-sh) ($n=10$). (**d**) Exogenous *FHL1* expression and the resultant decreased growth of AGS cells. Increased levels of *FHL1* expression were confirmed by qRT–PCR (left) and western blot (middle). Growth rates of cells with exogenous *FHL1* were shown to be significantly decreased (*$P<0.01$) (right).

distinguish the allelic origin of mRNA was not present. As qMSP detects only molecules that have dense methylation at primer sites, it was considered that it detected only densely methylated molecules, and methylation levels between 20 and 40% were observed in females.

In conclusion, we showed that *FHL1* on chromosome X is a methylation-silenced tumor-suppressor gene in gastrointestinal cancers, and its methylation in non-cancerous gastric mucosae contributes to the formation of an epigenetic field for cancerization.

MATERIALS AND METHODS

Cell lines and treatment with 5-aza-dC

Sixty-eight cancer cell lines (6 gastric, 7 colon, 12 lung, 12 skin, 7 pancreas, 4 esophageal, 4 prostate, 6 breast and 10 ovary cancer cell lines) and two normal colonic epithelial cells (CRL1790 and CRL1831) were obtained from the American Type Culture Collection (Manassas, VA, USA), Japanese Collection of Research Bioresources (Tokyo, Japan), RIKEN Cell Bank (Tsukuba, Japan) and Tohoku University Cell Resource Center for Biomedical Research (Sendai, Japan)(Supplementary Table 2). HSC39, HSC44 and HSC57 were gifted by Dr K Yanagihara; TMK1 was gifted by Dr W Yasui at Hiroshima University; and GC2 was established by MT For 5-aza-dC treatment. AGS and KATOIII cells were seeded on day 0; media containing freshly prepared 0.3 μM 5-aza-dC were added on days 1 and 3, and cells were harvested on day 5.[35]

Tissue specimens and analysis of *H. pylori* infection status

Cancer specimens were obtained from 80 male gastric cancer patients (average age = 60.4, range = 29–88) and 144 male colon cancer patients (average age = 70, range = 39–98) who underwent gastric and colon resection, respectively, with informed consent. All cancers were histologically diagnosed, and histological types of gastric cancers were classified according to the Lauren classification system (35 intestinal and 45 diffuse type).[36] EBV positivity was determined by *in situ* hybridization targeting *EBER1* using formalin-fixed and paraffin-embedded specimens.[37] The proportion of EBV-positive specimens (5 of 80, 6.3%) was close to EBV prevalence in a previous report (11 of 172, 6.4%).[38]

Normal-appearing gastric mucosae were obtained by endoscopic biopsy of the antral region from 60 healthy volunteers (32 male and 28 female; average age = 52, range = 25–91) and 70 gastric cancer patients

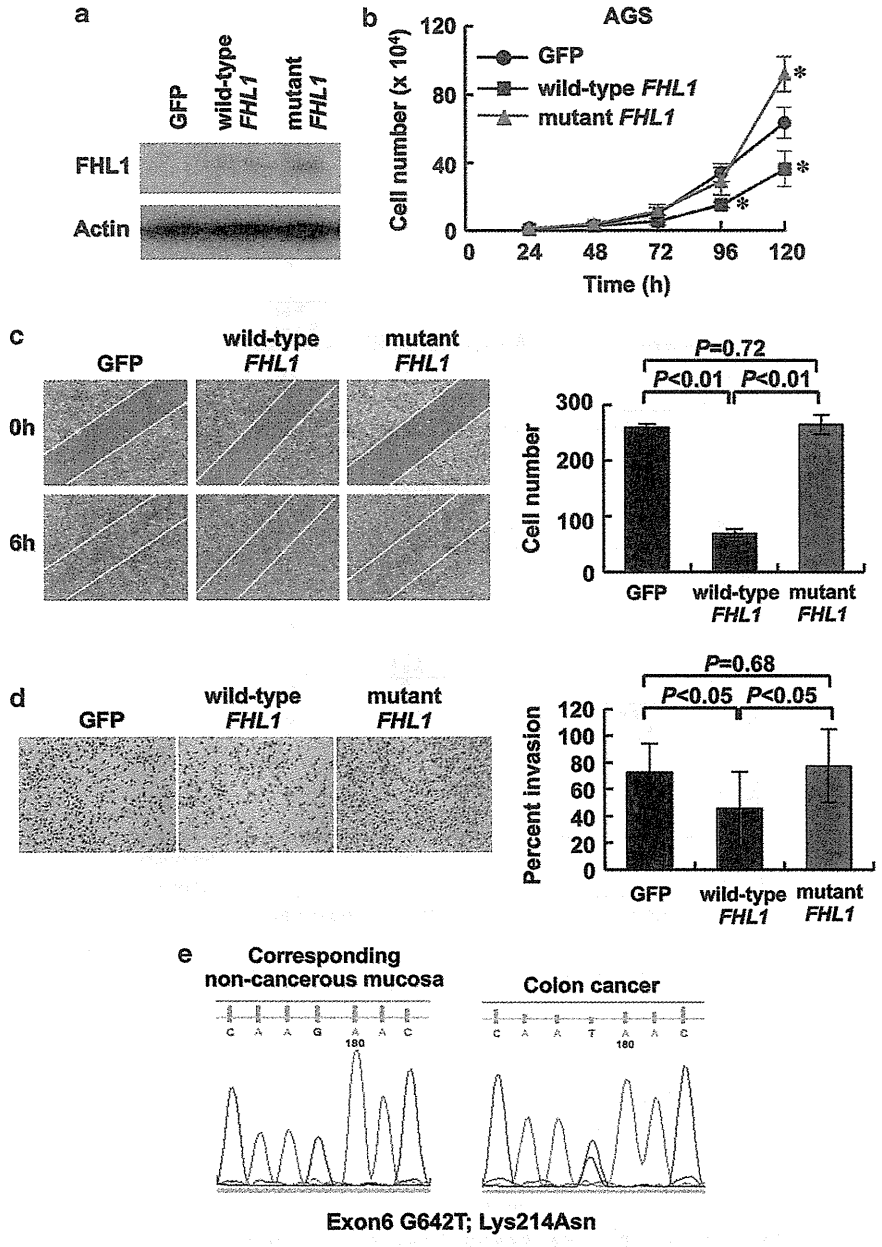

Figure 5. Inhibitory effects of *FHL1* on migration and invasion, and the lack of such functions in *FHL1* with the G642T mutation in AGS. (**a**) Expression levels of exogenous wild-type and mutant *FHL1* detected by western blot. (**b**) The growth-suppressive effect of the wild-type *FHL1*, and the lack of the effect in mutant *FHL1*. Whereas wild-type *FHL1* suppressed cell growth, mutant *FHL1* did not (*$P<0.01$). (**c**) Migration inhibition by wild-type *FHL1*, and the lack of the effect in the mutant *FHL1*. Whereas wild-type *FHL1* inhibited cell migration to 26.6% of the control cells, mutant *FHL1* did not. Photographs were taken at 0 and 6 h after scratching (left), and the number of cells that migrated into the scratched area was counted (mean ± s.d.; right). (**d**) Invasion inhibition by wild-type *FHL1*, and the lack of the effect in the mutant *FHL1*. Whereas wild-type *FHL1* inhibited cell invasion, mutant *FHL1* did not. Representative fields with invading cells on Matrigel-precoated membrane (left). Percent invasion is shown as the mean ± s.d. (right). (**e**) Sequence analysis of colon cancer specimens and corresponding non-cancerous colonic mucosae showed a somatic mutation (G642T; Lys214Asn) in exon 6 of *FHL1*.

(52 male and 18 female; average age = 65, range = 38–85). *H. pylori* infection status was analyzed by a serum anti-*H. pylori* IgG antibody test (SRL, Tokyo, Japan), rapid urease test (Otsuka, Tokushima, Japan) or culture test (Eiken, Tokyo, Japan). Gastric epithelial cells for qRT–PCR analysis were isolated by the gland isolation technique.[39] Normal-appearing colonic mucosae were obtained from a mucosal area distant from colon cancers of surgically resected specimens. Leukocytes were collected from one male (age = 47) and one female (age = 32) volunteer. Specimens were kept frozen at − 80 °C until DNA/RNA extraction. All the analyses using human-derived specimens were approved by the Institutional Review Boards.

Data processing of expression microarray analysis

Expression microarray analysis data in our previous report[19] were used. Signal intensities were scaled so that average signal intensity of all the 18 602 genes would become 500.

Sodium bisulfite modification, MSP, qMSP and bisulfite sequencing

Bisulfite modification was performed using 1 μg of *Bam*HI-digested genomic DNA as previously described.[40] MSP was performed with

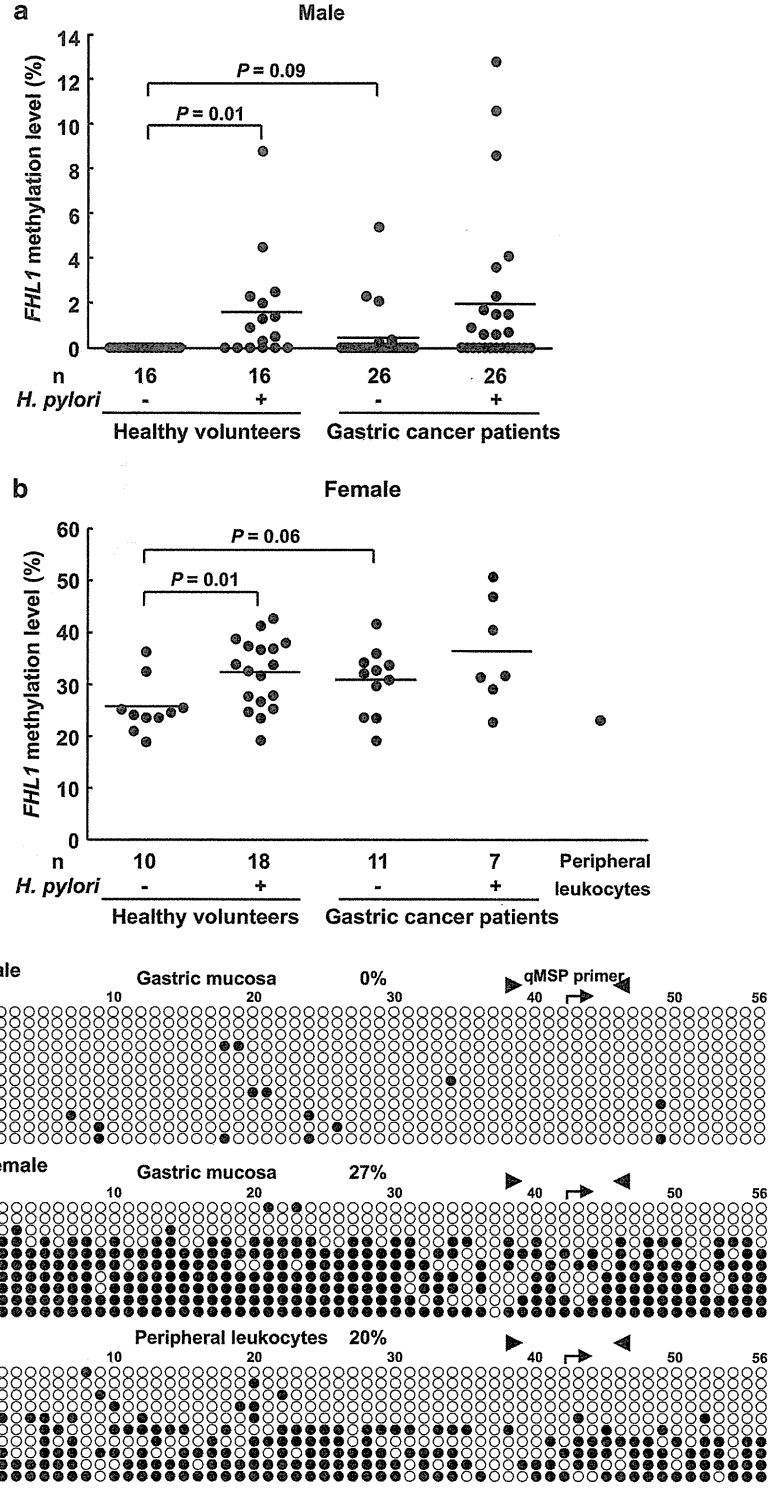

Figure 6. *FHL1* methylation levels in male and female gastric mucosae. (**a**) Methylation levels in male gastric mucosae of healthy volunteers and non-cancerous mucosae of gastric cancer patients. A horizontal line represents the mean methylation level for each group. Among healthy volunteers, *FHL1* methylation was present only in *H. pylori*-positive individuals ($P = 0.01$). Among individuals without *H. pylori* infection, *FHL1* methylation was present only in gastric cancer patients. (**b**) Methylation levels in female gastric mucosae and peripheral leukocytes. *FHL1* methylation levels distributed between 20 and 40%. Methylation levels were higher in *H. pylori*-positive healthy volunteers and gastric cancer patients also in female. (**c**) Bisulfite sequencing of male gastric mucosae, female gastric mucosae and female peripheral leukocytes. Female specimens contained both densely methylated and sparsely methylated DNA molecules, and it was considered that the inactive chromosome X can be densely and sparsely methylated. Closed circle, methylated CpG site; open circle, unmethylated CpG site; arrowheads, primers for qMSP; and arrow, transcription start site.

primer sets specific to methylated and unmethylated sequences (Supplementary Table 3). As controls, fully methylated and unmethylated DNA were prepared by methylating genomic DNA with *Sss*I methylase (New England Biolabs, Beverly, MA, USA) and by amplifying genomic DNA with the GenomiPhi amplification system (GE Healthcare, Buckinghamshire, UK), respectively.

Quantitative real-time MSP was performed by real-time PCR using SYBR Green I (BioWhittaker Molecular Applications, Rockland, ME, USA) and an iCycler Thermal Cycler (Bio-Rad Laboratories, Hercules, CA, USA). Although a primer set for MSP was also used for qMSP, a specific annealing temperature in the presence of SYBR Green I was determined (Supplementary Table 3). The number of molecules in a specimen was determined by comparing its amplification with those of standard DNA that contained known numbers of molecules (10^1–10^6 molecules). Based on the numbers of methylated (M) and unmethylated (U) molecules, a methylation level was calculated as the fraction of M molecules in the total number of DNA molecules (no. of M molecules + no. of U molecules). Standard DNA was prepared by cloning PCR products of methylated and unmethylated sequences into a vector (pGEM-T Easy, Promega, Madison, WI, USA). The CIMP status in a gastric cancer was determined as described previously.[27]

Bisulfite sequencing was conducted with primers common to methylated and unmethylated DNA sequences (Supplementary Table 4). The PCR product was cloned into pGEM-T Easy, and 10–12 clones were cycle-sequenced for each specimen.

qRT–PCR

cDNA was synthesized from 1 μg of total RNA using a Superscript III (Invitrogen, Carlsbad, CA, USA). qRT–PCR was performed by real-time PCR using SYBR Green I and an iCycler Thermal Cycler. Standard DNA was prepared by serial dilution of PCR products quantified by the QIAxcel system (QIAGEN, Valencia, CA, USA) after purification using Zymo-Spin I Columns (Zymo Research, Orange, CA, USA).[41] The measured number of cDNA molecules was normalized to that of b2-microglobulin (*b2MG*). The primers and PCR conditions are shown in Supplementary Table 5.

Knockdown and cDNA introduction assays

For a knockdown assay, two pairs and one pair of oligonucleotides were designed against *FHL1* and *Luciferase* (control), respectively (Supplementary Table 6). After annealing of sense and antisense oligonucleotides, the fragment was cloned into a pGreenPuro lentiviral vector (System Biosciences, Mountain View, CA, USA). For cDNA cloning, the entire coding region of human *FHL1* was amplified by RT–PCR (Supplementary Table 7), and cloned into a pCDH-CMV-MCS-EF1-Puro lentiviral vector (System Biosciences). As a control, *copGFP* was cloned into the vector in the same manner. The mutant cDNA was synthesized using the site-directed mutagenesis technique.[42] Using complementary primers carrying mutated sequence (mutation site forward and reverse primers; Supplementary Table 7) and primers for each end of the entire coding region (entire region reverse and forward primers), RT–PCR was performed to generate two DNA fragments that had overlapping ends. These two PCR products were combined by a subsequent PCR with primers for each end of the entire coding region to obtain the mutant cDNA. The mutant cDNA was cloned into a pCDH-CMV-MCS-EF1-Puro lentiviral vector.

The viral vectors and packaging vectors (pPACKH1 HIV Lentivector Packaging Kit, System Biosciences) were cotransfected into 293TN packaging cells, and culture media-containing pseudoviral particles were retrieved. Infection of cancer cell lines with pseudoviral particles was performed according to the manufacturer's protocol (System Biosciences), and stably expressing cells were selected by puromycin without cloning.

Cell growth, migration, invasion and apoptosis analysis

Cell growth was analyzed by seeding cells in triplicate in a six-well plate (3×10^4 cells, AGS; 1×10^5 cells, HSC39) and in a 12-well plate (5×10^3 cells, HCT116). Their numbers were counted at 24, 48, 72, 96 and 120 h. Three independent cultures were performed for one experiment.

Cell migration was analyzed by a wound-healing assay.[43] Cells were seeded in triplicate in a 6-cm dish coated with type I collagen (1×10^6 cells, AGS; 4×10^5 cells, MKN28), and cultured in RPMI-1640 medium containing 1% fetal calf serum to form a monolayer. The cell monolayer was scraped in a straight line with a pipette tip. After incubation for 6 and 12 h, the migrating cells were observed under bright-field microscopy. Three independent cultures were performed for one experiment.

Cell invasion was analyzed by a Matrigel invasion assay, using a Boyden chamber with the Matrigel-precoated membrane or Matrigel-free membrane in the top chamber (BD Biosciences, Bedford, MA, USA). Cells were seeded in top chambers in serum-free RPMI1640 (5×10^4 cells, AGS; 1×10^5 cells, MKN28), and the bottom chambers were filled with RPMI1640 containing 10% fetal calf serum. After incubation for 24 and 48 h (AGS and MKN28, respectively), the area of cells invading through the top chambers was measured by ImageJ software (version 1.38, National Institutes of Health, Bethesda, MD, USA). Percent invasion was calculated as the area of cells invading through the Matrigel-precoated membrane relative to those through Matrigel-free membrane. Three independent cultures were performed for one experiment and the experiment was repeated three times.

The apoptosis of the cells was analyzed by terminal deoxynucleotidyl transferase dUTP nick end labeling assay, using an *in situ* cell death detection kit, TMRred (Roche, Basel, Switzerland).

Tumor formation assay in nude mice

Cells (8×10^6 cells, HCT116) were inoculated subcutaneously on both flanks of 7-week-old male athymic nude mice (BALB/cAJc1-nu/nu; CLEA, Tokyo, Japan). Tumor sizes were measured with calipers every 3 days and the volume was calculated as (length × width^2) × 0.5, and tumor weights were measured at their killing on day 22. All the animal experiments were approved by the Animal Experiment Ethical Committee at the National Cancer Center.

Mutation analysis

All seven exons of *FHL1* were amplified using 100 ng of genomic DNA with primers located in introns, except for one primer on exon 7 (Supplementary Table 8). The PCR products were directly cycle-sequenced with a BigDye Terminator kit (PE Biosystems, Foster City, CA, USA) and an ABI PRISM 310 automated DNA sequencer (PE Biosystems).

Statistical analysis

Differences in mean methylation levels, expression levels, cell numbers and tumor sizes were analyzed by the Welch *t*-test. Association between *FHL1* methylation and clinicopathological factors was analyzed by the χ^2 test. All the analyses were performed using SPSS (SPSS, Inc., Chicago, IL, USA), and the results were considered significant when a P value <0.05 was obtained by two-sided tests.

CONFLICT OF INTEREST

The authors declare no conflict of interest.

ACKNOWLEDGEMENTS

We thank Dr Yanagihara and Dr Yasui for their kind gift of cell lines. This study was supported by a Grant-in-Aid for the Third-term Comprehensive Cancer Control Strategy from the Ministry of Health, Labour and Welfare, Japan, and by the National Cancer Center Research and Development Fund. TA is a recipient of the Research Resident Fellowship from the Foundation for Promotion of Cancer Research.

REFERENCES

1 Knudson AG. Two genetic hits (more or less) to cancer. *Nat Rev Cancer* 2001; **1**: 157–162.
2 Ushijima T. Detection and interpretation of altered methylation patterns in cancer cells. *Nat Rev Cancer* 2005; **5**: 223–231.
3 Jones PA, Baylin SB. The epigenomics of cancer. *Cell* 2007; **128**: 683–692.
4 Rivera MN, Kim WJ, Wells J, Driscoll DR, Brannigan BW, Han M *et al.* An X chromosome gene, WTX, is commonly inactivated in Wilms tumor. *Science* 2007; **315**: 642–645.
5 Zuo T, Wang L, Morrison C, Chang X, Zhang H, Li W *et al.* FOXP3 is an X-linked breast cancer suppressor gene and an important repressor of the HER-2/ErbB2 oncogene. *Cell* 2007; **129**: 1275–1286.
6 Wang L, Liu R, Li W, Chen C, Katoh H, Chen GY *et al.* Somatic single hits inactivate the X-linked tumor suppressor FOXP3 in the prostate. *Cancer Cell* 2009; **16**: 336–346.
7 Van Vlierberghe P, Palomero T, Khiabanian H, Van Der Meulen J, Castillo M, Van Roy N *et al.* PHF6 mutations in T-cell acute lymphoblastic leukemia. *Nat Genet* 2010; **42**: 338–342.

8 Maekita T, Nakazawa K, Mihara M, Nakajima T, Yanaoka K, Iguchi M *et al.* High levels of aberrant DNA methylation in Helicobacter pylori-infected gastric mucosae and its possible association with gastric cancer risk. *Clin Cancer Res* 2006; **12**: 989–995.
9 Ando T, Yoshida T, Enomoto S, Asada K, Tatematsu M, Ichinose M *et al.* DNA methylation of microRNA genes in gastric mucosae of gastric cancer patients: its possible involvement in the formation of epigenetic field defect. *Int J Cancer* 2009; **124**: 2367–2374.
10 Shen L, Kondo Y, Rosner GL, Xiao L, Hernandez NS, Vilaythong J *et al.* MGMT promoter methylation and field defect in sporadic colorectal cancer. *J Natl Cancer Inst* 2005; **97**: 1330–1338.
11 Kondo Y, Kanai Y, Sakamoto M, Mizokami M, Ueda R, Hirohashi S. Genetic instability and aberrant DNA methylation in chronic hepatitis and cirrhosis—a comprehensive study of loss of heterozygosity and microsatellite instability at 39 loci and DNA hypermethylation on 8 CpG islands in microdissected specimens from patients with hepatocellular carcinoma. *Hepatology* 2000; **32**: 970–979.
12 Ishii T, Murakami J, Notohara K, Cullings HM, Sasamoto H, Kambara T *et al.* Oesophageal squamous cell carcinoma may develop within a background of accumulating DNA methylation in normal and dysplastic mucosa. *Gut* 2007; **56**: 13–19.
13 Oka D, Yamashita S, Tomioka T, Nakanishi Y, Kato H, Kaminishi M *et al.* The presence of aberrant DNA methylation in noncancerous esophageal mucosae in association with smoking history: a target for risk diagnosis and prevention of esophageal cancers. *Cancer* 2009; **115**: 3412–3426.
14 Lee YC, Wang HP, Wang CP, Ko JY, Lee JM, Chiu HM *et al.* Revisit of field cancerization in squamous cell carcinoma of upper aerodigestive tract: better risk assessment with epigenetic markers. *Cancer Prev Res* 2011; **4**: 1982–1992.
15 Yan PS, Venkataramu C, Ibrahim A, Liu JC, Shen RZ, Diaz NM *et al.* Mapping geographic zones of cancer risk with epigenetic biomarkers in normal breast tissue. *Clin Cancer Res* 2006; **12**: 6626–6636.
16 Arai E, Kanai Y, Ushijima S, Fujimoto H, Mukai K, Hirohashi S. Regional DNA hypermethylation and DNA methyltransferase (DNMT) 1 protein overexpression in both renal tumors and corresponding nontumorous renal tissues. *Int J Cancer* 2006; **119**: 288–296.
17 Nakajima T, Maekita T, Oda I, Gotoda T, Yamamoto S, Umemura S *et al.* Higher methylation levels in gastric mucosae significantly correlate with higher risk of gastric cancers. *Cancer Epidemiol Biomarkers Prev* 2006; **15**: 2317–2321.
18 Ushijima T. Epigenetic field for cancerization. *J Biochem Mol Biol* 2007; **40**: 142–150.
19 Yamashita S, Tsujino Y, Moriguchi K, Tatematsu M, Ushijima T. Chemical genomic screening for methylation-silenced genes in gastric cancer cell lines using 5-aza-2′-deoxycytidine treatment and oligonucleotide microarray. *Cancer Sci* 2006; **97**: 64–71.
20 Ushijima T, Watanabe N, Shimizu K, Miyamoto K, Sugimura T, Kaneda A. Decreased fidelity in replicating CpG methylation patterns in cancer cells. *Cancer Res* 2005; **65**: 11–17.
21 Ding L, Wang Z, Yan J, Yang X, Liu A, Qiu W *et al.* Human four-and-a-half LIM family members suppress tumor cell growth through a TGF-beta-like signaling pathway. *J Clin Invest* 2009; **119**: 349–361.
22 Niu C, Liang C, Guo J, Cheng L, Zhang H, Qin X *et al.* Downregulation and growth inhibitory role of FHL1 in lung cancer. *Int J Cancer* 2012; **130**: 2549–2556.
23 Li X, Jia Z, Shen Y, Ichikawa H, Jarvik J, Nagele RG *et al.* Coordinate suppression of Sdpr and Fhl1 expression in tumors of the breast, kidney, and prostate. *Cancer Sci* 2008; **99**: 1326–1333.
24 Matsumoto M, Kawakami K, Enokida H, Toki K, Matsuda R, Chiyomaru T *et al.* CpG hypermethylation of human four-and-a-half LIM domains 1 contributes to migration and invasion activity of human bladder cancer. *Int J Mol Med* 2010; **26**: 241–247.
25 Sakashita K, Mimori K, Tanaka F, Kamohara Y, Inoue H, Sawada T *et al.* Clinical significance of loss of Fhl1 expression in human gastric cancer. *Ann Surg Oncol* 2008; **15**: 2293–2300.
26 Shen Y, Jia Z, Nagele RG, Ichikawa H, Goldberg GS. SRC uses Cas to suppress Fhl1 in order to promote nonanchored growth and migration of tumor cells. *Cancer Res* 2006; **66**: 1543–1552.
27 Enomoto S, Maekita T, Tsukamoto T, Nakajima T, Nakazawa K, Tatematsu M *et al.* Lack of association between CpG island methylator phenotype in human gastric cancers and methylation in their background non-cancerous gastric mucosae. *Cancer Sci* 2007; **98**: 1853–1861.
28 Ota N, Kawakami K, Okuda T, Takehara A, Hiranuma C, Oyama K *et al.* Prognostic significance of p16(INK4a) hypermethylation in non-small cell lung cancer is evident by quantitative DNA methylation analysis. *Anticancer Res* 2006; **26**: 3729–3732.
29 Matsusaka K, Kaneda A, Nagae G, Ushiku T, Kikuchi Y, Hino R *et al.* Classification of Epstein-Barr virus-positive gastric cancers by definition of DNA methylation epigenotypes. *Cancer Res* 2011; **71**: 7187–7197.
30 Ding L, Niu C, Zheng Y, Xiong Z, Liu Y, Lin J *et al.* FHL1 interacts with oestrogen receptors and regulates breast cancer cell growth. *J Cell Mol Med* 2011; **15**: 72–85.
31 Shathasivam T, Kislinger T, Gramolini AO. Genes proteins and complexes: the multifaceted nature of FHL family proteins in diverse tissues. *J Cell Mol Med* 2010; **14**: 2702–2720.
32 Achyut BR, Yang L. Transforming growth factor-beta in the gastrointestinal and hepatic tumor microenvironment. *Gastroenterol* 2011; **141**: 1167–1178.
33 Niwa T, Tsukamoto T, Toyoda T, Mori A, Tanaka H, Maekita T *et al.* Inflammatory Processes Triggered by Helicobacter pylori Infection Cause Aberrant DNA Methylation in Gastric Epithelial Cells. *Cancer Res* 2010; **70**: 1430–1440.
34 Panning B, Jaenisch R. RNA and the epigenetic regulation of X chromosome inactivation. *Cell* 1998; **93**: 305–308.
35 Moriguchi K, Yamashita S, Tsujino Y, Tatematsu M, Ushijima T. Larger numbers of silenced genes in cancer cell lines with increased de novo methylation of scattered CpG sites. *Cancer Lett* 2007; **249**: 178–187.
36 Lauren P. The two histological main types of gastric carcinoma: diffuse and so-called intestinal-type carcinoma. An attempt at a histo-clinical classification. *Acta Pathol Microbiol Scand* 1965; **64**: 31–49.
37 Fukayama M, Hayashi Y, Iwasaki Y, Chong J, Ooba T, Takizawa T *et al.* Epstein-Barr virus-associated gastric carcinoma and Epstein-Barr virus infection of the stomach. *Lab Invest* 1994; **71**: 73–81.
38 Luo B, Wang Y, Wang XF, Liang H, Yan LP, Huang BH *et al.* Expression of Epstein-Barr virus genes in EBV-associated gastric carcinomas. *World J Gastroenterol* 2005; **11**: 629–633.
39 Cheng H, Bjerknes M, Amar J. Methods for the determination of epithelial cell kinetic parameters of human colonic epithelium isolated from surgical and biopsy specimens. *Gastroenterol* 1984; **86**: 78–85.
40 Kaneda A, Kaminishi M, Sugimura T, Ushijima T. Decreased expression of the seven ARP2/3 complex genes in human gastric cancers. *Cancer Lett* 2004; **212**: 203–210.
41 Hosoya K, Yamashita S, Ando T, Nakajima T, Itoh F, Ushijima T. Adenomatous polyposis coli 1A is likely to be methylated as a passenger in human gastric carcinogenesis. *Cancer Lett* 2009; **285**: 182–189.
42 Ho SN, Hunt HD, Horton RM, Pullen JK, Pease LR. Site-directed mutagenesis by overlap extension using the polymerase chain reaction. *Gene* 1989; **77**: 51–59.
43 Liang CC, Park AY, Guan JL. *In vitro* scratch assay: a convenient and inexpensive method for analysis of cell migration *in vitro*. *Nat Protoc* 2007; **2**: 329–333.

Supplementary Information accompanies the paper on the Oncogene website (http://www.nature.com/onc)

Oncogene (2014) **33,** 2273–2278

www.nature.com/onc

SHORT COMMUNICATION

ANGPTL4 is a secreted tumor suppressor that inhibits angiogenesis

E Okochi-Takada[1], N Hattori[1], T Tsukamoto[2], K Miyamoto[3], T Ando[1,4], S Ito[5], Y Yamamura[5], M Wakabayashi[1], Y Nobeyama[1,6] and T Ushijima[1]

Tumor suppressors with extracellular function are likely to have advantages as targets for cancer therapy, but few are known. Here, we focused on angiopoietin-like 4 (ANGPTL4), which is a secreted glycoprotein involved in lipoprotein metabolism and angiogenesis, is methylation-silenced in human cancers, but has unclear roles in cancer development and progression. We found a deletion mutation in its coiled-coil domain at its N-terminal in human gastric cancers, in addition to hypermethylation of the *ANGPTL4* promoter CpG islands. Forced expression of wild-type *ANGPTL4*, but not *ANGPTL4* with the deletion, at physiological levels markedly suppressed *in vivo* tumorigenicity and tumor angiogenesis, indicating that the latter caused the former. Tumor-derived ANGPTL4 suppressed *in vitro* vascular tube formation and proliferation of human umbilical vascular endothelial cells, partly due to suppression of ERK signaling. These showed that ANGPTL4 is a genetically and epigenetically inactivated secreted tumor suppressor that inhibits tumor angiogenesis.

Oncogene (2014) **33,** 2273–2278; doi:10.1038/onc.2013.174; published online 20 May 2013

Keywords: epigenetics; angiogenesis; tumor suppressor; gastric cancer; DNA methylation

INTRODUCTION

Tumor-suppressor genes (TSGs) are somatically inactivated by genetic and/or epigenetic mechanisms.[1,2] Targeting TSGs for molecular target therapy has been attempted mainly for *p53*.[3,4] However, the attempts have not been easy, partly due to the fact that the *p53* gene product is neither a cell surface protein nor a typical enzyme.[5] Considering efficient delivery to targets, TSGs whose products function extracellularly as secreted proteins are likely to have advantages. So far, secreted frizzled-related proteins are known as secreted tumor suppressors,[6,7] but few others are known.

As a candidate, we previously identified that angiopoietin-like 4 (*ANGPTL4*), a member of the angiopoietin-like family, was silenced by aberrant DNA methylation of promoter CpG islands (CGIs) (methylation-silenced) in human cancers.[8,9] ANGPTL4 is a secreted glycoprotein, and is involved in lipoprotein metabolism through inhibition of lipoprotein lipase.[10] In contrast, the role of ANGPTL4 in angiogenesis remains controversial.[11–15] Likewise, its role in tumor formation also remains controversial—some reports suggesting its tumor-suppressive function[12,16,17] and others its oncogenic function.[18–20]

Here, we aimed to clarify the role of ANGPTL4 in cancer development and progression and also in tumor angiogenesis.

RESULTS AND DISCUSSION

Inactivation of *ANGPTL4* by epigenetic and genetic mechanisms in human gastric cancers

ANGPTL4 methylation was detected in 10 of 91 human gastric cancers (11%) by quantitative real-time methylation-specific PCR (Figure 1a). The mRNA and protein expression levels of ANGPTL4 in cancers with *ANGPTL4* methylation were significantly lower than those in cancers without methylation (Supplementary Figure S2). Methylation status did not have any association with clinicopathological features, but had a significant association with Epstein-Barr virus infection status and the presence of the CGI methylator phenotype[21] (Supplementary Figure S1 and Supplementary Table S1). In non-cancerous gastric mucosae of 71 gastric cancer patients and gastric mucosae of 58 healthy volunteers, the methylation level was also quantified. It was significantly higher in cancer patients than in healthy volunteers and in individuals with *H. pylori* infection than in those without (Figure 1b). This suggested the potential involvement of *ANGPTL4* methylation in the formation of an epigenetic field for cancerization, a predisposed normal-appearing tissue.[22]

ANGPTL4 mutation was then analyzed in 89 of the 91 gastric cancers (due to sample availability), and a somatic 21-bp deletion in exon 1 was identified in one specimen (cancer #217T) without *ANGPTL4* methylation (Figures 1c and d). ANGPLT4 consists of an N-terminal coiled-coil domain (CCD) and a C-terminal fibrinogen-like domain,[23,24] and the 21-bp deletion was located in the CCD (Supplementary Figure S3). The CCD is reported to be critical for regulation of the anti-angiogenic activity of ANGPTL4,[13] and the deletion here involved one of the two cysteine residues (Cys76 and Cys80) essential for the activity regulation by oligomerization.[25,26]

Loss of heterozygosity (LOH), which suggests the presence of a TSG,[27] was detected in 4 of 16 samples (25%) informative for a C/T polymorphism at the second position of codon 266. The locus of

[1]Division of Epigenomics, National Cancer Center Research Institute, Tokyo, Japan; [2]Oncological Pathology Division, Aichi Cancer Center Research Institute, Nagoya, Japan; [3]Division of Molecular Oncology, National Hospital Organization Kure Medical Center and Chugoku Cancer Center, Kureshi, Japan; [4] Third Department of Internal Medicine, University of Toyama, Toyama, Japan; [5]Department of Gastroenterological Surgery, Aichi Cancer Center Central Hospital, Nagoya, Japan and [6]Department of Dermatology, The Jikei University School of Medicine, Tokyo, Japan. Correspondence: Dr T Ushijima, Division of Epigenomics, National Cancer Center Research Institute, 5-1-1 Tsukiji, Chuo-ku, Tokyo 104-0045, Japan.
E-mail: tushijim@ncc.go.jp
Received 27 September 2012; revised 14 February 2013; accepted 28 March 2013; published online 20 May 2013

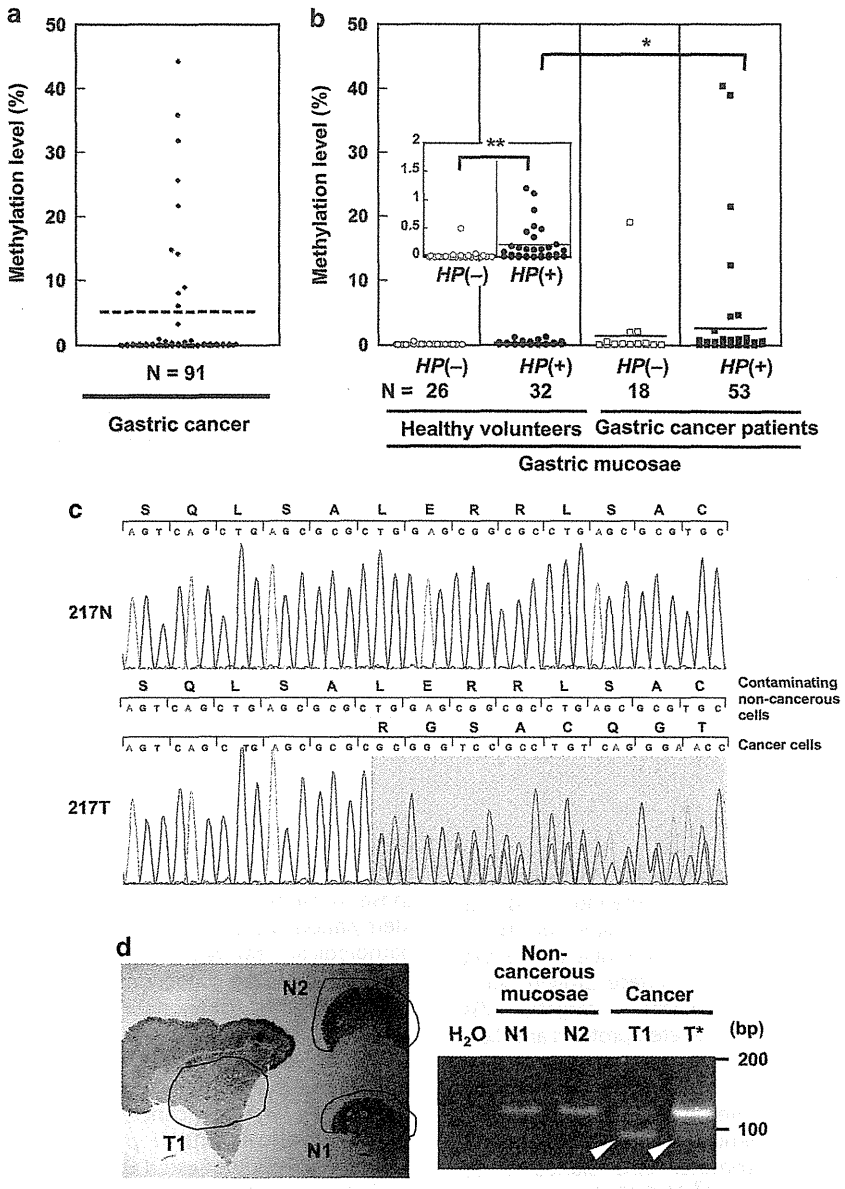

Figure 1. Aberrant methylation and a mutation of *ANGPTL4* in human gastric cancers, and methylation in non-cancerous gastric mucosae. (**a**) *ANGPTL4* methylation levels in gastric cancer specimens. Cancer samples were obtained from 91 gastric cancer patients undergoing gastrectomy with informed consents and approval by the institutional review boards. Some of the samples and methylation data were obtained from our previous study.[33] Quantitative real-time methylation-specific PCR was conducted with sodium bisulfite-treated DNA and primer sets specific to methylated and unmethylated sequences (Supplementary Table S2). Using a cutoff value of 6% (broken line), as in previous studies,[34–36] 10 cancer specimens were considered to have aberrant methylation. (**b**) *ANGPTL4* methylation levels in gastric mucosae of 58 healthy volunteers (30 male and 28 female; average age = 55 years) and 71 non-cancerous gastric mucosae of gastric cancer patients (50 male and 21 female; average age = 67 years) obtained by endoscopic biopsy of the antral region. *H. pylori* infection status was analyzed by a serum anti-*H. pylori* IgG antibody test (SRL, Tokyo, Japan), rapid urease test (Otsuka, Tokushima, Japan) or culture test (Eiken, Tokyo, Japan). The methylation level in gastric mucosae was significantly higher in gastric cancer patients than in healthy volunteers. The mean methylation level is shown by a horizontal line. $^{*}P<0.05$, $^{**}P<0.01$ (the unpaired Welch's *t*-test, two-sided). (**c**) A deletion mutation in a human gastric cancer specimen. All the seven exons and splice donor/acceptor sites of *ANGPTL4* were amplified by PCR (Supplementary Table S2), and the PCR products were directly cycle sequenced. The sequences of a gastric cancer specimen (217T) and its corresponding non-cancerous tissue (217N) between nucleotides 385 and 423 are shown. A 21-bp deletion in exon 1 was detected (shown in the gray background). (**d**) Confirmation of the deletion mutation using DNA samples obtained from a single tissue section. A 117-bp region encompassing the deletion was amplified by PCR, and the deletion was detected as a PCR product with a shorter size (96 bp). DNA from the cancer (T1), but not that from non-cancerous areas (N1 and N2), yielded the shorter product (shown by arrows). T*, genomic DNA extracted from frozen tumor tissues. If LOH was present in T1, the band intensity ratio was expected to be 1:1 (wild type:deletion mutant) (fraction of cancer cells was pathologically assessed to be 61–67%). If LOH was not present, it was expected to be 2:1. The ratio observed was ~1:2, and LOH was considered to be present in T1.

ANGPTL4, 19p13.3, has been suggested to contain TSGs, due to frequent LOH of the region in several types of cancers, such as pancreatic and colon cancers.[28–30] In addition, two human gastric cancer cell lines (MKN28 and AGS) without *ANGPTL4* expression had methylation of its promoter, and their treatment with 5-aza-2′-deoxycytidine (5-aza-dC), a DNA methylation inhibitor,

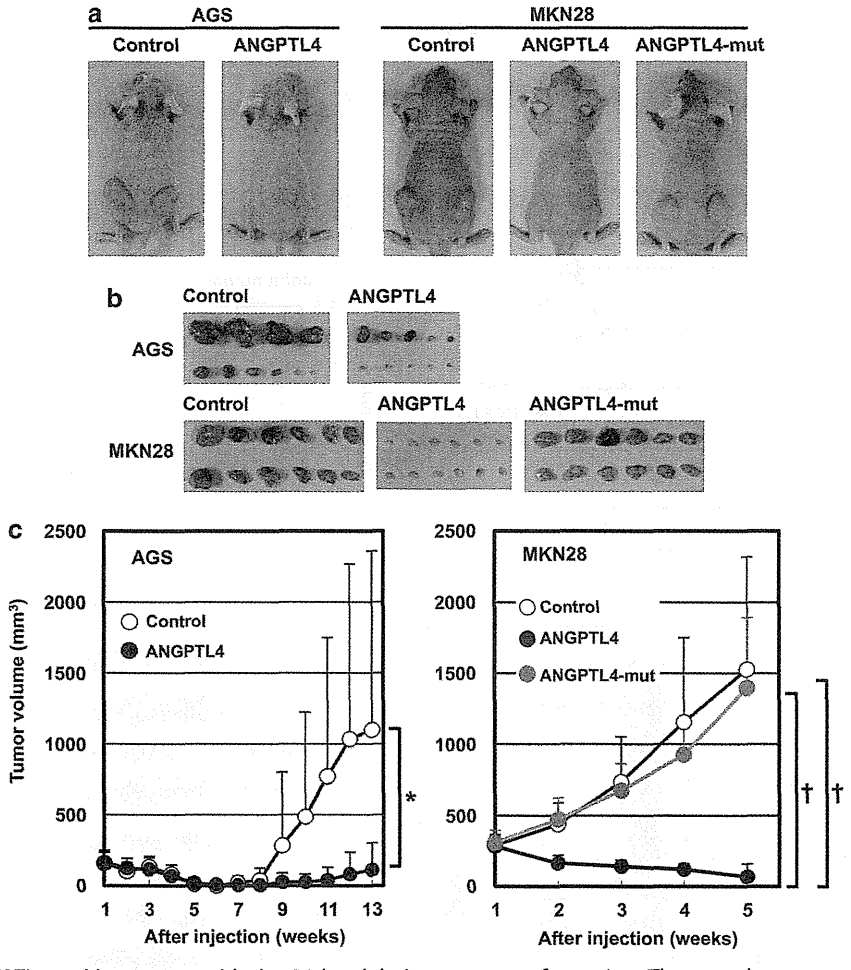

Figure 2. The effect of *ANGPTL4* and its mutant with the 21-bp deletion on tumor formation. The complementary DNA of wild-type *ANGPTL4*, its mutant with the deletion, and *EGFP* as a control were inserted into a mammalian expression vector pIRESpuro3 with the human cytomegalovirus immediate early promoter (Clontech, Mountain View, CA, USA). Individual vectors were transfected into MKN28 or AGS gastric cancer cell lines, and transfectants were selected with puromycin (0.3 μg/ml). Athymic nude mice (BALB/cAJc1-nu/nu, CLEA, Tokyo, Japan) were subcutaneously injected with cells (1×10^7 cells) mixed with an equal volume of Matrigel (BD Biosciences, San Diego, CA, USA). All the animal experiments were approved by the Committee for Ethics in Animal Experimentation, and conducted in accordance with the Guidelines for Animal Experiments of the National Cancer Center. (**a**) Representative photographs of transplanted tumors at 13 weeks (AGS) and 5 weeks (MKN28). *ANGPTL4* markedly suppressed tumor formation, while its mutant with the deletion lacked the activity. (**b**) Macroscopic views of the tumors resected at 13 weeks (AGS) and at 5 weeks (MKN28). Introduction of *ANGPTL4* markedly suppressed tumor sizes in both cell lines. The variable degree of suppression in AGS might have been due to the lower ANGPTL4 expression level (Supplementary Figure S5c). (**c**) Tumor growth curves after the injection. The volume of tumor (mm^3) was calculated by the formula: (length × $width^2$)/2. A tumor volume is shown as a mean ± s.d. ($N = 10$ in AGS and $N = 12$ in MKN28). $^*P < 0.05$, $^\dagger P < 0.001$ (Student's *t*-test).

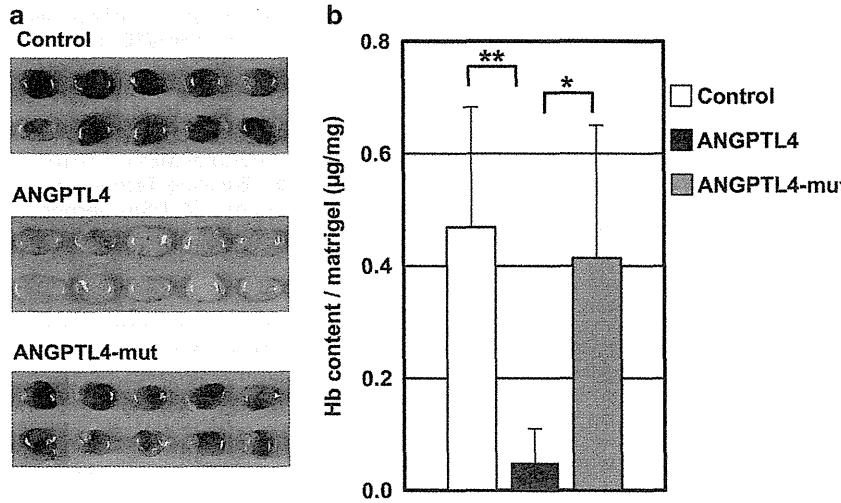

Figure 3. For caption please see page 2276.